
DOMAIN-SPECIFIC RISK MINIMIZATION FOR OUT-OF-DISTRIBUTION GENERALIZATION

Yi-Fan Zhang¹, Jindong Wang², Jian Liang¹, Zhang Zhang¹, Baosheng Yu³,
 Liang Wang¹, Dacheng Tao³, Xing Xie²

¹Institute of Automation, Chinese Academy of Sciences

²Microsoft Research Asia, ³The University of Sydney.

ABSTRACT

Recent domain generalization (DG) approaches typically use the hypothesis learned on source domains for inference on the unseen target domain. However, such a hypothesis can be arbitrarily far from the optimal one for the target domain, induced by a gap termed “adaptivity gap”. Without exploiting the domain information from the unseen test samples, adaptivity gap estimation and minimization are intractable, which hinders us to robustify a model to any unknown distribution. In this paper, we first establish a generalization bound that explicitly considers the adaptivity gap. Our bound motivates two strategies to reduce the gap: the first one is ensembling multiple classifiers to enrich the hypothesis space, then we propose effective gap estimation methods for guiding the selection of a better hypothesis for the target. The other method is minimizing the gap directly by adapting model parameters using online target samples. We thus propose **Domain-specific Risk Minimization (DRM)**. During training, DRM models the distributions of different source domains separately; for inference, DRM performs online model steering using the source hypothesis for each arriving target sample. Extensive experiments demonstrate the effectiveness of the proposed DRM for domain generalization with the following advantages: 1) it significantly outperforms competitive baselines on different distributional shift settings; 2) it achieves either comparable or superior accuracies on all source domains compared to vanilla empirical risk minimization; 3) it remains simple and efficient during training, and 4) it is complementary to invariant learning approaches.

1 INTRODUCTION

Machine learning models generally suffer from degraded performance when the training and test data are non-IID (independently and identically distributed). To overcome the brittleness of classical empirical risk minimization (ERM), there is an emerging trend of developing out-of-distribution (OOD) generalization approaches (Muandet et al., 2013; Li et al., 2018b), where models trained on multiple source domains/datasets can be directly deployed on *unseen* target domains. Various OOD frameworks are proposed, e.g., disentanglement (Zhang et al., 2022a), causal invariance (Arjovsky et al., 2019), and adversarial training (Ganin et al., 2016; Li et al., 2018c).

Existing approaches might rely on two strong assumptions. (i) **Hypothesis over-confidence**. Most works directly apply a source-trained hypothesis to *any* unseen target domains (Arjovsky et al., 2019; Krueger et al., 2021; Rame et al., 2022) by implicitly assuming that *the training hypothesis space contains an ideal target hypothesis*. However, the IID and OOD performances are not always positively correlated (Teney et al., 2022), i.e., the optimal hypothesis on source domains might not perform well on any target domains. The distance between the optimal source and target hypothesis is termed *adaptivity gap* (Dubey et al., 2021), which is even shown can be arbitrarily large (Chu et al., 2022). (ii) **Pessimistic adaptivity gap reduction**. Although the adaptivity gap is ubiquitous, it is almost impossible to identify and minimize due to the unavailability of OOD target samples. As a consequence, there exists no approach that can tackle *all* kinds of distribution shifts at once (e.g., diversity shift in PACS (Li et al., 2017) and correlation shift in the Colored MNIST (Arjovsky et al., 2019)), but only a specific kind (Ye et al., 2022). In a word, it is almost impossible to robustify a model to arbitrarily unknown distribution shift *without* utilizing the target samples during inference.

The two disadvantages are also neglected by the commonly-used domain adaptation and generalization bounds (Ben-David et al., 2010; Albuquerque et al., 2020; Zhao et al., 2019), which mostly ignore the terms that are related to the target domain. To this end, we introduce a new generalization bound that does not depend on the choice of hypothesis space and explicitly considers the adaptivity gap between source and target. The bound motivates two possible test-time adaptation strategies: the first one is to train specific classifiers for different source domains, and then dynamically ensemble them, which is shown able to enrich the set of the hypothesis space (Domingos, 1997). The other is to utilize the arriving target samples, namely once a target sample is given, we update the model by its provided target domain information. To summarize, this paper makes the following contributions:

- **A novel perspective.** We provide a new generalization bound that does not depend on the choice of hypothesis space and explicitly considers the adaptivity gap between source domains and the target domain. Our bound is shown tighter than the existing one and provides intuition for reweighting methods, test-time adaptation methods, and classifier ensembling methods for good domain generalization performance.
- **A new approach.** We propose a new Domain-specific Risk Minimization (DRM) method, which consists of two components: (i) During training, DRM constructs specific classifiers for source domains and is trained by reweighting empirical loss. (ii) During the test, DRM performs test-time model selection and retraining for each target sample. Thus, the source classifiers are dynamically changed for each target data and we can enrich the support set of the hypothesis space in this way to minimize the adaptivity gap directly.
- **Extensive experiments.** We perform extensive experiments on popular OOD benchmarks showing that DRM (1) achieves very competitive generalization performance on both diversity shift benchmarks and correlation shift benchmarks; (2) beats most existing test-time adaptation methods with a large margin; (3) is orthogonal to other DG methods; (4) reserves strong recognition capability on source domains, and (5) is parameter-efficient and converges even faster than ERM thanks to the structure.

2 RELATED WORK

Domain adaptation and domain generalization Domain/Out-of-distribution generalization (Muandet et al., 2013; Zhang et al., 2021b; Li et al., 2018c; Zhang et al., 2022b) aims to learn a model that can extrapolate well in unseen environments. Representative methods like Invariant Risk Minimization (IRM) (Arjovsky et al., 2019) concentrates on the objective of extracting data representations that lead to invariant prediction across environments under a multi-environment setting. In this paper, we emphasize the importance of considering adaptivity gap and use online target data for adaptation, without an invariance strategy, the proposed DRM can attain superior generalization capacity.

Ensemble learning in domain generalization learn ensembles of multiple specific models for different source domains to improve the generalization ability, e.g., domain-specific neural networks layer (Ding & Fu, 2017), domain-specific classifiers (Wang et al., 2020), and domain-specific batch normalization (Segu et al., 2020). Domain-specific classifiers are also used in this work, however, empirical results show that directly ensembling multiple classifiers with a uniform weight degrades the performance and the proposed DRM can attain superior generalization results in contrast.

Test-time adaptive methods are recently proposed to utilize target samples. Test-time Training methods need to design proxy tasks during tests such as self-consistence (Zhang et al., 2021c), rotation prediction (Sun et al., 2020) and need extra models; Test-time adaptation methods adjust model parameters based on unsupervised objectives such as entropy minimization (Wang et al., 2021) or update a prototype for each class (Iwasawa & Matsuo, 2021). Domain-adaptive method (Dubey et al., 2021) needs extra models for adapting to the target domain. Our generalization bound indicates that these methods can explicitly reduce the target loss upper bound. And in this paper, we propose other ways to perform test-time adaptation, i.e., multi-classifier dynamic combination and retraining.

3 A BOUND BY CONSIDERING ADAPTIVITY GAP

Let $\mathcal{X}, \mathcal{Y}, \mathcal{Z}$ denote the input, output, and feature space, respectively. We use X, Y, Z to denote the random variables taking values from $\mathcal{X}, \mathcal{Y}, \mathcal{Z}$, respectively. In the DG setting, we have access to a

labeled training dataset that consists of several different but related training distributions (domains): $\mathcal{D} = \bigcup_{i=1}^K \mathcal{D}_i$, where K is the number of domains. Each \mathcal{D}_i corresponds to a joint distribution $P_i(X, Y)$ with a optimal classifier $f_i : \mathcal{X} \rightarrow [0, 1]$ ¹. We focus on a deterministic setting where the output $Y = f_i(X)$ is given by a deterministic classifier, f_i , which varies from domain to domain. Let $g : \mathcal{X} \rightarrow \mathcal{Z}$ and $h : \mathcal{Z} \rightarrow \{0, 1\}$ denote the encoder/feature transformation and the prediction head, respectively. The error incurred by hypothesis $\hat{f} := h \circ g$ under domain \mathcal{D}_i can be defined as $\epsilon_i(\hat{f}) = \mathbb{E}_{X \sim \mathcal{D}_i} [|\hat{f}(X) - f_i(X)|]$. Given f_i and \hat{f} as binary classification functions, we have

$$\epsilon_i(\hat{f}) = \epsilon_i(\hat{f}, f_i) = \mathbb{E}_{X \sim \mathcal{D}_i} [|\hat{f}(X) - f_i(X)|] = P_{X \sim \mathcal{D}_i}(\hat{f}(X) \neq f_i(X)). \quad (1)$$

Existing analysis on OOD Existing popular approaches on OOD focus on learning invariant representations (Li et al., 2018b; Ganin et al., 2016) with the following theoretical intuition.

Proposition 1. (Adapted from (Ben-David et al., 2006)) Denote $\tilde{\mathcal{D}}$ as the induced distribution over feature space \mathcal{Z} for every distribution \mathcal{D} over raw space. Here we use \mathcal{H} as a hypothesis space defined on feature space, i.e., $\mathcal{H} \subseteq \{h : \mathcal{Z} \rightarrow \{0, 1\}\}$. Define \mathcal{D}_i as a source distribution over \mathcal{X} , which enables a mixture construction of source domains as $\mathcal{D}_\alpha = \sum_{i=1}^K \alpha_i \mathcal{D}_i(\cdot)$. Denote a fictitious distribution $\mathcal{D}_\mathcal{T}^\alpha = \sum_{i=1}^K \alpha_i^* \mathcal{D}_i(\cdot)$ as the convex combination of source domains which is the closest to $\mathcal{D}_\mathcal{T}$, where $\alpha_1^*, \dots, \alpha_K^* = \arg \min_{\alpha_1, \dots, \alpha_K} d_{\mathcal{H}}(\mathcal{D}_\mathcal{T}, \sum_{i=1}^K \alpha_i \mathcal{D}_i(\cdot))$. The fictitious distribution induces a feature space distribution $\tilde{\mathcal{D}}_\mathcal{T}^\alpha = \sum_{i=1}^K \alpha_i^* \tilde{\mathcal{D}}_i(\cdot)$. The following inequality holds for the risk $\epsilon_\mathcal{T}(\hat{f})$ on target domain $\mathcal{D}_\mathcal{T}$ (See appendix C.1 for derivations and explanations):

$$\epsilon_\mathcal{T}(\hat{f}) \leq \lambda_\alpha + \sum_{i=1}^K \alpha_i \epsilon_i(\hat{f}) + d_{\mathcal{H}}(\tilde{\mathcal{D}}_\mathcal{T}^\alpha, \tilde{\mathcal{D}}_\alpha) + d_{\mathcal{H}}(\tilde{\mathcal{D}}_\mathcal{T}, \tilde{\mathcal{D}}_\mathcal{T}^\alpha), \quad (2)$$

where a feature transformation g is learned such that the induced source distributions on \mathcal{Z} are close to each other and a prediction head h over the feature space \mathcal{Z} is to achieve small empirical errors on source domains. The bound depends on the risk of the optimal hypothesis λ_α , namely. the hypothesis space contains an optimal classifier that performs well on both the source and the target domains.

Adaptivity gap The above assumption cannot be guaranteed to hold true under all scenarios and is usually intractable to compute for most practical hypothesis spaces, making the bound conservative and loose. Besides, even if we have the optimal classifier, it is almost impossible to find the optimal one using given source domains. The reason is that the classifier trained by the average risk across domains can lie far from the optimal classifier for a target domain (Dubey et al., 2021; Chu et al., 2022), induced by adaptivity gap:²

Definition 1 (Adaptivity gap). *The adaptivity gap between \mathcal{D}_i and the target domain $\mathcal{D}_\mathcal{T}$ can be formally defined as $\mathbb{E}_{\mathcal{D}_\mathcal{T}}[|f_i - f_\mathcal{T}|]$, namely the error incurred by using f_i for inference in $\mathcal{D}_\mathcal{T}$.*

A failure case of invariant representation. We construct a simple counterexample where invariant representations fail to generalize. As shown in Figure 1, given the following four domains: $\mathcal{D}_o \sim \mathcal{N}([-3, 3], I)$, $\mathcal{D}_g \sim \mathcal{N}([3, 3], I)$, $\mathcal{D}_r \sim$

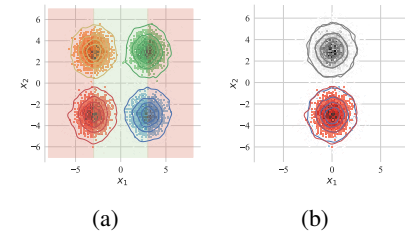


Figure 1: A failure case of invariant representations for domain generalization. (a) Four domains in different colors: orange, green, red and blue. (b) Invariant representations learnt from domain \mathcal{D}_r and \mathcal{D}_b . The grey color indicates the transformed target domains.

¹Most theories and examples in this paper considers binary classification for easy understanding and can be easily extended to multi-class classification.

²The adaptivity gap is NOT the same as labeling functions difference (Zhao et al., 2019), where the latter measures the difference of two hypotheses: $\min\{\mathbb{E}_{\mathcal{D}_i}[|f_i - f_\mathcal{T}|], \mathbb{E}_{\mathcal{D}_\mathcal{T}}[|f_i - f_\mathcal{T}|]\}$. However, the error of target hypothesis $f_\mathcal{T}$ on the source domain is intractable to estimate and meaningless for DG (Kpotufe & Martinet, 2018). The definition of adaptivity gap directly measures if the source classifier performs well on the target.

$\mathcal{N}([-3, -3], I)$, $\mathcal{D}_b \sim \mathcal{N}([3, -3], I)$, where $X = (x_1, x_2)$ and

$$f_o(X) = \begin{cases} 0 & \text{if } x_1 \leq -3 \\ 1 & \text{otherwise} \end{cases}, f_r(X) = \begin{cases} 0 & \text{if } x_1 \leq -3 \\ 1 & \text{otherwise} \end{cases}, f_g(X) = \begin{cases} 1 & \text{if } x_1 \leq 3 \\ 0 & \text{otherwise} \end{cases}, f_b(X) = \begin{cases} 1 & \text{if } x_1 \leq 3 \\ 0 & \text{otherwise} \end{cases}, \quad (3)$$

where I indicates the identity matrix. Then, the optimal hypothesis $f^*(X) = 1$ iff $x_1 \in (-3, 3)$ achieves perfect classification on all domains. Let $\mathcal{D}_r, \mathcal{D}_b$ denote source domains and $\mathcal{D}_o, \mathcal{D}_g$ denote target domains. Given hypothesis $\hat{f} := h \circ g$ where the feature transformation function is $g(X) = \mathbb{I}_{x_1 < 0} \cdot (x_1 + 3) + \mathbb{I}_{x_1 > 0} \cdot (x_1 - 3)$ in Figure 1 (b), namely, the invariant representation of $\mathcal{D}_r, \mathcal{D}_b$ is learnt, which is $\mathcal{D}_{rb} = g \circ \mathcal{D}_b = g \circ \mathcal{D}_r = \mathcal{N}([0, -3], I)$. However, the labeling functions f_r of \mathcal{D}_r and f_b of \mathcal{D}_b are just the reverse such that $f_r(X) = 1 - f_b(X); \forall X \in \mathcal{D}_{rb}$. In this case, according to Eq. 1, we have:

$$\begin{aligned} \epsilon_{rb}(\hat{f}) &= \epsilon_r(h \circ g) + \epsilon_b(h \circ g) = P_{X \sim g \circ \mathcal{D}_r}(h(X) \neq f_r(X)) + P_{X \sim g \circ \mathcal{D}_b}(h(X) \neq f_b(X)) \\ &= 1 - P_{X \sim \mathcal{D}_{rb}}(h(X) \neq f_b(X)) + P_{X \sim \mathcal{D}_{rb}}(h(X) \neq f_b(X)) = 1 \end{aligned} \quad (4)$$

Therefore, the invariant representation leads to large joint errors on all source and target domains for any prediction head h without considering the adaptivity gap. Motivated by this, we provide a tighter OOD upper bound that considers the adaptivity gap.

Proposition 2. *Let $\{\mathcal{D}_i, f_i\}_{i=1}^K$ and \mathcal{D}_T, f_T be the empirical distributions and corresponding labeling function for source and target domain, respectively. For any hypothesis $\hat{f} \in \mathcal{H}$, given mixed weights $\{\alpha_i\}_{i=1}^K; \sum_{i=1}^K \alpha_i = 1, \alpha_i \geq 0$, we have:*

$$\epsilon_T(\hat{f}) \leq \sum_{i=1}^K \left(\mathbb{E}_{X \sim \mathcal{D}_i} \left[\alpha_i \frac{P_T(X)}{P_i(X)} |\hat{f} - f_i| \right] + \alpha_i \mathbb{E}_{\mathcal{D}_T} [|f_i - f_T|] \right). \quad (5)$$

The two terms on the right-hand side have natural interpretations: the first term is the weighted source errors, and the second one measures the distance between the labeling functions from the source domain and target domain. Compared to Eq. 2, Eq. 5 does not depend on λ_α , i.e., the choice of the hypothesis class \mathcal{H} makes no difference. More importantly, the new upper bound in Eq. 5 reflects the influence of adaptivity gaps between each source domain to the target, i.e., $\mathbb{E}_{\mathcal{D}_T} [|f_i - f_T|]$. The most similar generalization bound to us is (Albuquerque et al., 2019), in Appendix C.3, we show that the proposed bound is tighter. Although in this work, the density ratio $P_T(x)/P_i(x)$ is ignored and regarded as a constant, it has an interesting connection between reweighting methods.

Connection to reweighting methods. Intuitively, the density ratio stresses the importance of data sample reweighting, where data samples that are more likely from the target domain should have larger weights. Existing methods (Liu et al., 2021a; Zhang et al., 2022b; Sagawa et al., 2020) use similar reweighting strategies and our error bound provides a theoretical explanation for why they work well on DG (See Appendix C.4 for formal definition and derivation).

4 DOMAIN-SPECIFIC RISK MINIMIZATION

Our error bound suggests a novel perspective on OOD algorithm design: DRM. DRM avoids the calculation of untractable terms in Eq. 5 and approximately minimizes the bound.

4.1 DOMAIN-SPECIFIC LABELING FUNCTION

One natural idea is to use **domain-specific** classifiers $\{\hat{f}_i\}_{i=1}^K$ rather than a shared classifier \hat{f} for source domains. Each \hat{f}_i is responsible for classification in \mathcal{D}_i . In the training phase, our goal is to minimize $\frac{1}{K} \sum_{i=1}^K \mathbb{E}_{x \sim \mathcal{D}_i} [|\hat{f}_i - f_i|]$ by assuming that K training domains are uniformly mixed ($\alpha_i = 1/K$). The generalization results are better with reweighting terms, e.g., using GroupDRO (Sagawa et al., 2020), in the RotatedMNIST dataset, the accuracy of $d = 5$ with reweighting terms is 97.3%, which is better than 96.8% without reweighting. We simply ignore the reweighting term in this work since it is not our focus.

Specifically, given K source domains, DRM utilizes a *shared* encoder g and a group of prediction head $\{h_i\}_{i=1}^K$ for all domains, respectively. The encoder is trained by all data samples while each

head h_i is trained by images from domain \mathcal{D}_i . It is also possible (but less efficient and accurate) to use specific g_i for each domain.³

4.2 TEST-TIME MODEL SELECTION AND ADAPTATION

Test-time adaptive intuitions from the bound. After training, we can get K hypotheses \hat{f}_i that can well approximate source labeling functions. During testing, our error bound provides two strategies to minimize the second term in the upper bound, i.e., $\sum_{i=1}^K \alpha_i \mathbb{E}_{\mathcal{D}_T} [|f_i - f_T|]$. One natural strategy is to find $\alpha^* = \arg \min \alpha_i \mathbb{E}_{\mathcal{D}_T} [|f_i - f_T|]$, which is termed **test-time model selection**. The intuition is that if we can find the source domain \mathcal{D}_{i^*} with a labeling function f_{i^*} that minimizes the adaptivity gap $\mathbb{E}_{\mathcal{D}_T} [|f_{i^*} - f_T|]$, then we have that $\alpha_i = 1$, iff $i = i^*$, otherwise 0 will minimize this term. Second, if we suppose $\hat{f}_i \approx f_i$, then minimizing $\sum_{i=1}^K \mathbb{E}_{\mathcal{D}_T} [\hat{f}_i - f_T]$ will also minimize the bound. The resulting strategy is termed **test-time retraining**. Since f_T is unknown, we can update model parameters by the inferred target pseudo labels or use some unsupervised losses such as entropy minimization. Note that these two strategies are orthogonal and can be used simultaneously. In the following, we articulate these two strategies.

4.2.1 TEST-TIME MODEL SELECTION

As mentioned above, we can manipulate α_i to affect the second term in our bound: for every test sample $x \in \mathcal{D}_T$, if we can estimate the adaptivity gap $\{H_i = |f_i(x) - f_T(x)|\}_{i=1}^K$ and choose $i^* = \arg \min \{H_i\}_{i=1}^K$. Then $\alpha_i = 1$, iff $i = i^*$, otherwise 0 makes this term the minimum and the prediction will be $\hat{f}_{i^*}(x)$. The challenge is estimating $\{H_i\}_{i=1}^K$ and we propose two approximations.

Similarity Measurement (SM). We first reformulate $\alpha_i \mathbb{E}_{\mathcal{D}_T} [|f_i - f_T|]$ as follows:

$$\begin{aligned} \alpha_i \mathbb{E}_{\mathcal{D}_T} [|f_i - f_T|] &= \alpha_i \mathbb{E}_{\mathcal{D}_T} [|f_i - \mathbb{E}_{\mathcal{D}_i} [f_i] + \mathbb{E}_{\mathcal{D}_i} [f_i] - f_T|] \\ &\leq \alpha_i (\mathbb{E}_{\mathcal{D}_T} [|f_i - \mathbb{E}_{\mathcal{D}_i} [f_i]|] + \mathbb{E}_{\mathcal{D}_T} [|\mathbb{E}_{\mathcal{D}_i} [f_i] - f_T|]), \end{aligned} \quad (6)$$

where f_T is intractable and we then focus on $\mathbb{E}_{\mathcal{D}_T} [|f_i - \mathbb{E}_{\mathcal{D}_i} [f_i]|]$, which intuitively measures the prediction difference of the given test data $x \in \mathcal{D}_T$ and the average prediction result in domain \mathcal{D}_i . However, taking the average of the prediction labels might produce ill-posed results⁴ and we use $\mathbb{E}_{\mathcal{D}_T} [|g - \mathbb{E}_{\mathcal{D}_i} [g]|]$ to approximate this term, where we calculate the representation difference between the test sample and the average representation of the domain \mathcal{D}_i . For each $x \in \mathcal{D}_T$, the estimation $H_i = \text{Dist}(g(x), \mathbb{E}_{\mathcal{D}_i} [g])$, i.e., the distance between $g(x)$ and the average representation of \mathcal{D}_i . The Dist function can be any distance metric such as l_p -Norm, the negative of cosine similarity, f -divergence (Nowozin et al., 2016), MMD (Li et al., 2018b), or \mathcal{A} -distance (Ben-David et al., 2010). We use cosine similarity (CSM) and l_2 -Norm (L2SM) in our experiments for simplicity.

Prediction Entropy Measurement (PEM). During testing, denote the K individual classification logits as $\{\bar{\mathbf{y}}^k\}_{k=1}^K$, where $\bar{\mathbf{y}}^k = [y_1^k, \dots, y_C^k]$, and C is the number of classes. Given the following assumption: “*the more confident prediction $h_i \circ g$ makes on \mathcal{D}_T , the more similar f_i and f_T will be*”. Then, the prediction entropy of $\bar{\mathbf{y}}^k$ can be calculated as $H_k = - \sum_{i=1}^c \frac{y_i^k}{\sum_{j=1}^c y_j^k} \log \frac{y_i^k}{\sum_{j=1}^c y_j^k}$, where the entropy is used as our expected estimation. In our experiments, we find that the prediction entropy is consistent with domain similarities, which is similar to SM.

Model Ensembling. A one-hot mixed weight is too deterministic and cannot fully utilize all learned classifiers. **Softing mixed weights**, on the other hand, can further boost generalization performance and enlarge the hypothesis space, i.e., for ERM, we can generate the final prediction as $\sum_{k=1}^K \bar{\mathbf{y}}_k H_k^{-\gamma} / \sum_{i=1}^K H_i^{-\gamma}$, where $H_k^{-\gamma}$ indicates the contribution of each classifier. We use $-\gamma$, but not γ since the smaller the adaptivity gap, the larger the contribution of f_i should be. Specifically, for

³Using domain-specific g_i will inevitably increase the computation and memory burden. We observe that $h_i \circ g$ gives an OOD accuracy of 70.1% while the result is only 64.8% for $h_i \circ g_i$ on the Colored MNIST dataset. A possible reason is that a shared encoder g can be seen as an implicit regularization, which prevents the model from overfitting specific domains.

⁴If all source domains have two data samples with different labels, e.g., two different one-hot labels $[0, 1]$, $[1, 0]$. Then the average prediction result of all source domains will be $[0.5, 0.5]$ and have no difference.

$\gamma = 0$, we then have a uniform combination, i.e., $\alpha_i = 1/K, \forall i \in [1, 2, \dots, K]$; for $\gamma \rightarrow \infty$, we then have a one-hot weight vector with $\alpha_i = 1$ iff $i = i^*$ otherwise 0. Refer to Appendix Algorithm 1,2 for the detail of the training and test pipelines of the proposed two selection strategies. In experiments, we compare the different selection strategies and PEM generally performs the best, thus we later use PEM as the default choice.

4.2.2 TEST-TIME RETRAINING

The simplest idea to retrain the model is that, for each prediction head, we use the argmax of the prediction result as pseudo labels and then train the model by cross-entropy loss, which is termed *Vanilla Retraining*. However, it performs poorly (Table 1) no matter only tuning the prediction heads (Clf) or the overall model (Full). Thanks to the domain-specific classifiers, we can produce more reliable pseudo labels. Specifically, we generate pseudo labels by the weighted mix of predictions by all heads where the weights are just mixed weights in the model selection phase. We compare these generation strategies on the PACS dataset with ‘A’ as the target. Table 1 shows that with the proposed pseudo-label generation strategy, the retraining process can be well guided.

Remark. By modeling domain-specific labeling functions, DRM can further reduce source errors (i.e., the first term in our upper bound); For the second term, the test-time model selection and retraining reduce the adaptivity gap by enriching hypothesis class and target sample retraining. In Appendix B, we show that by directly minimizing the adaptivity gap, the proposed DRM performs well on the counterexample in Section 3.

5 EXPERIMENTAL RESULTS

We first conduct case studies on a popular **correlation shift** dataset (Colored MNIST). Then, we compare DRM with other advanced methods on DG benchmarks (**diversity shift**). The results verify the argument in the introduction: by utilizing the target data during test, we can better robustify a model to both distribution shifts. We also compare DRM with different test-time adaptive methods with various backbones. For fair comparisons, We use test-time retraining just when compared to test-time adaptation methods, namely **DRM denotes the method wo/ retraining by default**.

Experimental Setup. We use five popular OOD generalization benchmark datasets: Colored MNIST (Arjovsky et al., 2019), Rotated MNIST (Ghifary et al., 2015), PACS (Li et al., 2017), VLCS (Torralba & Efros, 2011), and DomainNet (Peng et al., 2019). We compare our model with ERM (Vapnik, 1999), IRM (Arjovsky et al., 2019), Mixup (Yan et al., 2020), MLDG (Li et al., 2018a), CORAL (Sun & Saenko, 2016), DANN (Ganin et al., 2016), CDANN (Li et al., 2018c), MTL (Blanchard et al., 2021), SagNet (Nam et al., 2021), ARM (Zhang et al., 2021a), VREx (Krueger et al., 2021), RSC (Huang et al., 2020), Fish (Shi et al., 2022), and Fishr (Rame et al., 2022). All the baselines in DG tasks are implemented using the codebase of Domainbed (Gulrajani & Lopez-Paz, 2021). See Appendix E for datasets and implementation details.

5.1 CASE STUDIES ON CORRELATION SHIFT DATASETS

In the following, we conduct thorough experiments and analysis of a popular correlation shift benchmark, i.e., the ColoredMNIST dataset (Arjovsky et al., 2019). It constructs a binary classification problem based on the MNIST dataset (digits 0-4 are class one and 5-9 are class two). Digits in the dataset are either colored red or green, and there is a strong correlation between color and label but the correlations vary across domains. For example, green digits have a 90% chance of belonging to class 1 in the first domain $+90\%(d = 0)$, and a 10% chance of belonging to class 1 in the third domain $-90\%(d = 2)$.

DRM has superior generalization ability on the dataset with correlation shift. As shown in Table 2, ERM achieves high accuracies on training domains but below-chance accuracy on the test domain due to its reliance on spurious correlations. IRM (Arjovsky et al., 2019) forms a tradeoff between training and testing accuracy. An ERM model trained on only gray images, i.e., ERM (gray), is perfectly invariant by construction and attains a better tradeoff than IRM. The upper

Table 1: Comparison between different pseudo label generalization strategies.

Method	Clf	Full
ERM	80.3	80.3
DRM wo/ retraining	83.0	83.0
Vanilla retraining	83.0	83.8
DRM retraining	84.1	84.8

Table 2: **Accuracies (%) of different methods on training/testing domains for the Colored MNIST synthetic task.** OIM (optimal invariant model) and RG (random guess) are hypothetical mechanisms.

Method	+90% ($d = 0$)		+80% ($d = 1$)		-90% ($d = 2$)		Avg	
	train	test	train	test	train	test	train	test
ERM	86.1\pm3.9	71.8 \pm 0.4	83.6 \pm 0.5	72.9 \pm 0.1	87.5 \pm 3.4	28.7 \pm 0.5	85.7	57.8
IRM	78.2 \pm 9.5	72.0 \pm 0.1	70.6 \pm 9.1	72.5 \pm 0.3	85.3 \pm 4.7	58.5\pm3.3	78.0	67.7
DRM	81.8 \pm 9.8	86.7\pm2.4	90.2 \pm 0.2	80.6 \pm 0.2	88.0 \pm 4.5	43.1 \pm 7.5	86.7	70.1
DRM+CORAL	83.4 \pm 8.6	85.3 \pm 2.3	91.6\pm0.7	80.7\pm0.2	89.4\pm4.9	47.2 \pm 3.6	88.1	71.1
RG	50	50	50	50	50	50	50	50
OIM	75	75	75	75	75	75	75	75
ERM (gray)	84.8 \pm 2.7	73.9 \pm 0.3	84.3 \pm 1.4	73.7 \pm 0.4	83.4 \pm 2.3	73.8 \pm 0.7	84.2	73.8

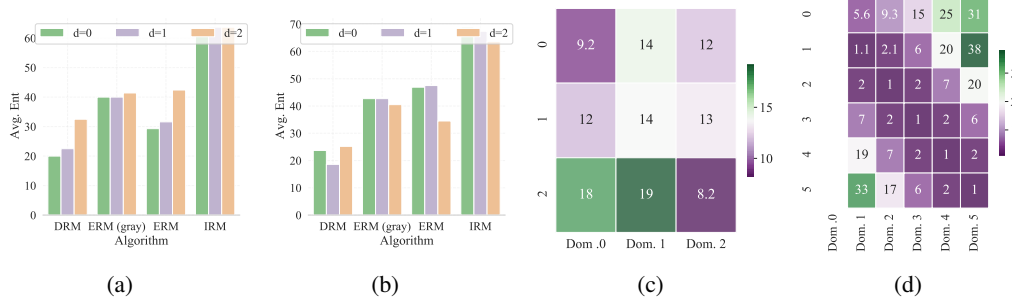


Figure 2: **The entropy of different predictions.** (a) Training domain $\{0, 1\}$ and testing domain $\{2\}$. (b) The average of training/testing domains $\{0, 1\}/\{2\}$, $\{0, 2\}/\{1\}$, and $\{1, 2\}/\{0\}$. (c) Domain-classifier correlation matrix, the value v_{ij} is the entropy of predictions incurred by predicting samples in the domain i with classifier j . Dom. i indicates the classifier for the domain $d = i$. (d) Domain-classifier correlation matrices on Rotated MNIST.

bound performance of invariant representations (OIM) is a hypothetical model that not only knows all spurious correlations but also has no modeling capability limit. For averaged generalization performance, DRM, without any invariance regularization, outperforms IRM by a large margin ($> 2.4\%$). Besides, *the source accuracy of DRM is even higher than ERM and significantly higher than IRM and OIM*. Note that DRM is complementary with invariant learning-based methods, where incorporating CORAL (Sun & Saenko, 2016) can further boost both training and testing performances. Though the Colored MNIST dataset is a good indicator to show the model capacity for avoiding spurious correlation, these spurious correlations are unrealistic and utopian. Therefore, when testing on large DG benchmarks, ERM outperforms IRM. Different from them, DRM not only performs well on the semi-synthetic dataset but also attains state-of-the-art performance on large benchmarks.

PEM implicitly reduces prediction entropy and the entropy-based strategy performs well in finding a proper labeling function for inference. The prediction entropy is often related to the fact that more confident predictions tend to be correct (Wang et al., 2021). Figure 2(a) shows that the entropy in target domain ($d = 2$) tends to be greater than the entropy in source domains, where the source domain with stronger spurious correlations ($d = 1$) also has larger entropy than easier one ($d = 0$). Fortunately, with the entropy minimization strategy, we can find the most confident classifier for a given data sample, and DRM can reduce the prediction entropy (Figure 2(b)). To further analyze the entropy minimization strategy, we visualize the domain-classifier correlation matrix in Figure 2(c), where the entropy between the domain and its corresponding classifier is minimal, verifying the efficacy of the entropy minimization strategy.

5.2 RESULTS ON GENERAL OOD BENCHMARKS

OOD results. The average OOD results on all benchmarks are shown in Table 3. We observe consistent improvements achieved by DRM compared to existing algorithms. The results indicate the superiority of DRM in real-world diversity shift datasets. See Appendix for multi-target domain generalization and the detailed performance on every domain.

Table 3: Out-of-distribution generalization performance.

Method	CMNIST	RMNIST	VLCS	PACS	DomainNet	Avg
ERM (Vapnik, 1999)	57.8 \pm 0.2	97.8 \pm 0.1	77.6 \pm 0.3	86.7 \pm 0.3	41.3 \pm 0.1	72.2
IRM (Arjovsky et al., 2019)	67.7 \pm 1.2	97.5 \pm 0.2	76.9 \pm 0.6	84.5 \pm 1.1	28.0 \pm 5.1	70.9
CORAL (Sun & Saenko, 2016)	58.6 \pm 0.5	98.0 \pm 0.0	77.7 \pm 0.2	87.1 \pm 0.5	41.8 \pm 0.1	72.6
MTL (Blanchard et al., 2021)	57.6 \pm 0.3	97.9 \pm 0.1	77.7 \pm 0.5	86.7 \pm 0.2	40.8 \pm 0.1	72.1
SagNet (Nam et al., 2021)	58.2 \pm 0.3	97.9 \pm 0.0	77.6 \pm 0.1	86.4 \pm 0.4	40.8 \pm 0.2	72.2
ARM (Zhang et al., 2021a)	63.2 \pm 0.7	98.1 \pm 0.1	77.8 \pm 0.3	85.8 \pm 0.2	36.0 \pm 0.2	72.2
VREx (Krueger et al., 2021)	67.0 \pm 1.3	97.9 \pm 0.1	78.1 \pm 0.2	87.2 \pm 0.6	30.1 \pm 3.7	72.1
Fish (Shi et al., 2022)	61.8 \pm 0.8	97.9 \pm 0.1	77.8 \pm 0.6	85.8 \pm 0.6	43.4 \pm 0.3	73.3
Fishr (Rame et al., 2022)	68.8 \pm 1.4	97.8 \pm 0.1	78.2 \pm 0.2	86.9 \pm 0.2	41.8 \pm 0.2	74.7
DRM	70.1 \pm 2.0	98.1 \pm 0.2	80.5 \pm 0.3	88.5 \pm 1.2	42.4 \pm 0.1	75.9
DRM+CORAL	62.7 \pm 1.3	98.3 \pm 0.1	79.5 \pm 2.4	88.4 \pm 0.9	42.7 \pm 0.1	76.0

Table 4: In-distribution performance on VLCS and PACS.

Method	VLCS					PACS				
	C	L	S	V	Avg	A	C	P	S	Avg
ERM	78.2 \pm 3.3	87.8 \pm 9.0	86.3 \pm 10.2	83.3 \pm 11.6	83.9	96.7 \pm 0.3	96.4 \pm 1.5	95.3\pm1.2	96.3\pm0.1	96.2
IRM	76.9 \pm 2.9	88.2\pm8.9	85.3 \pm 9.8	77.3 \pm 1.0	81.9	95.9 \pm 1.6	94.2 \pm 2.5	94.3 \pm 1.0	94.5 \pm 1.8	94.7
DRM	78.5\pm2.9	87.2 \pm 9.2	87.3\pm9.0	84.0\pm10.9	84.3	96.9\pm0.3	96.4\pm1.3	95.2 \pm 0.9	96.1 \pm 0.6	96.2

In-distribution results. Current DG methods ignore the performance of source domains since they focus on target results. However, source domain performance is also of great importance in real-world applications (Yang et al., 2021), i.e., the in-distribution performance. We then show the in-distribution performances of VLCS and PACS in Table 4, and other domains are in Table 11. DRM achieves comparable or superior performance on source domains compared to ERM and beats IRM by a large margin, which indicates that DRM achieves satisfying in- and out-distribution performance.

Table 5: Comparison of our method and existing test-time adaptation methods on PACS. The reported number is the average generalization performance over P, A, C, S four domains.

Method	BSZ=32	BSZ=8
ResNet50	83.98	83.98
PLClf	85.63	85.55
PLFull	86.50	85.88
SHOT	86.53	85.85
SHOTIM	86.40	85.68
T3A	86.23	86.00
ResNet50w/ BN	83.18	83.18
TentClf	84.15	84.15
TentNorm	85.60	84.00
DRM	86.57	86.57
+Retrain Cls	87.90	87.83
+Retrain Full	89.30	89.33

Table 6: Domain generalization accuracy with different backbone networks on PACS. The reported number is the average generalization performance over P, A, C, S four domains.

Method	BSZ=32	BSZ=8
ResNet18	79.98	79.98
DRM	80.30	80.30
+Retrain Cls	82.95	82.18
+Retrain Full	84.70	84.35
ResNet50	83.98	83.98
DRM	86.57	86.57
+Retrain Cls	87.90	87.83
+Retrain Full	89.30	89.33
ViT-B16	87.10	87.10
DRM	87.85	87.85
+Retrain Cls	90.08	90.08
+Retrain Full	90.95	90.85

Comparison with test-time adaptation methods. For fair comparisons, following (Iwasawa & Matsuo, 2021), the base models (ERM and DRM) are trained only on the default hyperparameters and without the fine-grained parametric search. Because (Gulrajani & Lopez-Paz, 2021) omits the BN layer from pre-trained ResNet when fine-tuning on source domains, we cannot simply use BN-based methods on the ERM baseline. For these methods, their baselines are additionally trained on ResNet-50 with BN. Models with the highest IID accuracy are selected and all test-time adaptation methods are applied to improve the generalization performance. The baselines include Tent (Wang et al., 2021), T3A (Iwasawa & Matsuo, 2021), pseudo labeling (PL) (Lee et al., 2013), SHOT (Liang et al., 2020), and SHOT-IM (Liang et al., 2020). For methods that use gradient backpropagation, we implement both update the prediction head (Clf) and full model (Full). Results in Table 5 show that: (i) Simply retraining the classifier or the full model by its own prediction is comparable to existing methods; (ii) Tent (Wang et al., 2021) is sensitive to batch size but the proposed DRM is not; (iii) The performance of DRM without retraining attains comparable results compared to existing methods,

Table 7: Comparison of different test-time model selection strategies on the PACS dataset.

Method	A	C	P	S	Avg
DRM w/ Uniform weight	81.2 ± 2.2	71.2 ± 1.2	93.7 ± 0.3	78.6 ± 1.5	81.2
DRM w/ CSM	83.0 ± 2.1	74.6 ± 2.5	95.6 ± 0.8	80.4 ± 1.2	83.4
DRM w/ NNM	85.5 ± 2.4	76.8 ± 2.0	96.6 ± 0.4	81.8 ± 1.5	85.2
DRM w/ L2SM	87.7 ± 1.7	80.0 ± 0.5	96.0 ± 1.6	82.1 ± 1.2	86.5
DRM w/ PEM	88.3 ± 2.9	80.1 ± 0.8	97.0 ± 0.5	80.9 ± 0.7	86.6

and when incorporated by the proposed retraining method, the performance beats all baselines by a large margin.

Results of various backbones. We conduct experiments with various backbones in Table 6, including ResNet-50, ResNet-18, and Vision Transformers (ViT-B16). DRM achieves consistent performance improvements compared to ERM. Specifically, DRM improves 5.3%, 4.7%, and 3.9% for ResNet-50, ResNet-18, and ViT-B16 with evaluation batch size (BSZ) 32, respectively.

5.3 ABLATION STUDIES AND ANALYSIS

Different model selection strategies. Here we also conduct another baseline termed **Neural Network Measurement (NNM)**. To fully utilize the modeling capability of the neural network, we propose estimating $\alpha_i \mathbb{E}_{\mathcal{D}_T} [\|f_i - f_T\|]$ by NN. Specifically, during training, a domain discriminator is trained to classify which domain is each image from. During test, for $x \in \mathcal{D}_T$, the prediction result of the discriminator will be $\{d_i\}_{i=1}^K$, and $\{H_i = -d_i\}_{i=1}^K$ is used as the estimation. We compare all the proposed strategies and a simple ensembling learning baseline, which uses a uniform weight for classifier ensembling. Table 7 shows that simple ensembling method works poorly in all domains. In contrast, the proposed methods achieve consistent improvements and PEM generally performs best.

Correlation matrix. From the correlation matrices, we find that: (i) The entropy of predictions between one source domain and its corresponding classifier is minimal. (ii) On the target domain, classifiers cannot attain very low entropy as they attained on the corresponding source domains. (iii) The entropy of predictions has a certain correlation with domain similarity. For example, in Figure 2(d), classifier for domain $d = 1$ (with rotation angle 15°) attains the minimum entropy on the unseen target domain $d = 0$ (no rotation). As the rotation angle increases, the entropy also increases. This phenomenon also occurs in other domains. Refer to the appendix for more analysis.

Model complexity. As shown in Table 8, methods that require manipulating gradients (Fish (Shi et al., 2022)) or following the meta-learning pipeline (ARM (Zhang et al., 2021a)) have much slower training speed compared to ERM. The proposed DRM, without the need for aligning representations (Ganin et al., 2016), matching gradient (Shi et al., 2022), or learning invariant representations (Arjovsky et al., 2019), has a training speed that is faster than most existing DG methods, especially on small datasets RotatedMNIST. The training speed of DRM is slower than ERM because of training additional classifiers. See appendix for more comparison.

Convergence analysis. The training dynamics of DRM and several baselines on PACS dataset are shown in Figure 3, where $d = 0$ is the target domain. IRM is unstable and hard to converge. ARM follows a meta-learning pipeline and converges slowly. In contrast, DRM converges even faster than ERM.

6 CONCLUDING REMARKS

We theoretically and empirically study the importance of the adaptivity gap for domain generalization. Inspired by our the-

Table 8: Comparisons of different methods on the number of parameters and training time on RotatedMNIST.

Method	Time (sec)	Params (M)
ERM	168.32	0.3546
IRM	236.80	0.3546
ARM	360.69	0.4562
FISH	251.76	0.3546
DRM	203.15	0.3595

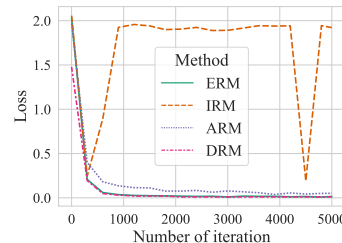


Figure 3: Loss curves.

ory, we propose DRM to eliminate the negative effects brought by adaptivity gap. DRM achieve great performance in both OOD and ID settings. We hope that our results can shed new light on the model design for domain generalization problems. One possible direction is to estimate $\alpha_i P_{\mathcal{T}}(x)/P_i(x)$ and then reweight data samples. Besides, the additional parameters incurred by the multi-classifiers structure can be reduced by advanced techniques and model designs, e.g., varying coefficient technique (Nie et al., 2020; Hastie & Tibshirani, 1993).

REFERENCES

Isabela Albuquerque, João Monteiro, Mohammad Darvishi, Tiago H Falk, and Ioannis Mitliagkas. Generalizing to unseen domains via distribution matching. *arXiv preprint arXiv:1911.00804*, 2019.

Isabela Albuquerque, João Monteiro, Mohammad Darvishi, Tiago H Falk, and Ioannis Mitliagkas. Adversarial target-invariant representation learning for domain generalization. In *Arxiv*, 2020.

Martin Arjovsky, Léon Bottou, Ishaan Gulrajani, and David Lopez-Paz. Invariant risk minimization. *arXiv preprint arXiv:1907.02893*, 2019.

Shai Ben-David, John Blitzer, Koby Crammer, and Fernando Pereira. Analysis of representations for domain adaptation. In *NIPS*, 2006.

Shai Ben-David, John Blitzer, Koby Crammer, Alex Kulesza, Fernando Pereira, and Jennifer Wortman Vaughan. A theory of learning from different domains. *Machine learning*, 2010.

Aharon Ben-Tal, Laurent El Ghaoui, and Arkadi Nemirovski. *Robust Optimization*. Princeton university press, 2009.

Gilles Blanchard, Aniket Anand Deshmukh, Ürün Dogan, Gyemin Lee, and Clayton Scott. Domain generalization by marginal transfer learning. *J. Mach. Learn. Res.*, 2021.

Xu Chu, Yujie Jin, Wenwu Zhu, Yasha Wang, Xin Wang, Shanghang Zhang, and Hong Mei. Dna: Domain generalization with diversified neural averaging. In *International Conference on Machine Learning*, pp. 4010–4034. PMLR, 2022.

Erick Delage and Yinyu Ye. Distributionally robust optimization under moment uncertainty with application to data-driven problems. *Operations research*, 2010.

Zhengming Ding and Yun Fu. Deep domain generalization with structured low-rank constraint. *IEEE Transactions on Image Processing*, 27(1):304–313, 2017.

Pedro M Domingos. Why does bagging work? a bayesian account and its implications. In *KDD*, pp. 155–158. Citeseer, 1997.

Abhimanyu Dubey, Vignesh Ramanathan, Alex Pentland, and Dhruv Mahajan. Adaptive methods for real-world domain generalization. In *Proceedings of the IEEE/CVF Conference on Computer Vision and Pattern Recognition*, pp. 14340–14349, 2021.

Yaroslav Ganin, Evgeniya Ustinova, Hana Ajakan, Pascal Germain, Hugo Larochelle, François Laviolette, Mario Marchand, and Victor Lempitsky. Domain-adversarial training of neural networks. *The journal of machine learning research*, 17(1):2096–2030, 2016.

Muhammad Ghifary, W Bastiaan Kleijn, Mengjie Zhang, and David Balduzzi. Domain generalization for object recognition with multi-task autoencoders. In *ICCV*, 2015.

Ishaan Gulrajani and David Lopez-Paz. In search of lost domain generalization. In *ICLR*, 2021.

Trevor Hastie and Robert Tibshirani. Varying-coefficient models. *Journal of the Royal Statistical Society: Series B (Methodological)*, 55(4):757–779, 1993.

Zhaolin Hu and L Jeff Hong. Kullback-leibler divergence constrained distributionally robust optimization. Available at *Optimization Online*, 2013.

Zeyi Huang, Haohan Wang, Eric P Xing, and Dong Huang. Self-challenging improves cross-domain generalization. In *ECCV*, 2020.

Yusuke Iwasawa and Yutaka Matsuo. Test-time classifier adjustment module for model-agnostic domain generalization. *Advances in Neural Information Processing Systems*, 34:2427–2440, 2021.

Samory Kpotufe and Guillaume Martinet. Marginal singularity, and the benefits of labels in covariate-shift. In *Conference On Learning Theory*, pp. 1882–1886. PMLR, 2018.

David Krueger, Ethan Caballero, Joern-Henrik Jacobsen, Amy Zhang, Jonathan Binas, Dinghuai Zhang, Remi Le Priol, and Aaron Courville. Out-of-distribution generalization via risk extrapolation (rex). In *ICML*, 2021.

Dong-Hyun Lee et al. Pseudo-label: The simple and efficient semi-supervised learning method for deep neural networks. In *Workshop on challenges in representation learning, ICML*, 2013.

Da Li, Yongxin Yang, Yi-Zhe Song, and Timothy M Hospedales. Deeper, broader and artier domain generalization. In *ICCV*, 2017.

Da Li, Yongxin Yang, Yi-Zhe Song, and Timothy Hospedales. Learning to generalize: Meta-learning for domain generalization. In *AAAI*, 2018a.

Haoliang Li, Sinno Jialin Pan, Shiqi Wang, and Alex C Kot. Domain generalization with adversarial feature learning. In *CVPR*, 2018b.

Ya Li, Xinmei Tian, Mingming Gong, Yajing Liu, Tongliang Liu, Kun Zhang, and Dacheng Tao. Deep domain generalization via conditional invariant adversarial networks. In *ECCV*, 2018c.

Jian Liang, Dapeng Hu, and Jiashi Feng. Do we really need to access the source data? source hypothesis transfer for unsupervised domain adaptation. In *International Conference on Machine Learning*, pp. 6028–6039. PMLR, 2020.

Evan Z Liu, Behzad Haghgoo, Annie S Chen, Aditi Raghunathan, Pang Wei Koh, Shiori Sagawa, Percy Liang, and Chelsea Finn. Just train twice: Improving group robustness without training group information. In *International Conference on Machine Learning (ICML)*, 2021a.

Xiaofeng Liu, Bo Hu, Linghao Jin, Xu Han, Fangxu Xing, Jinsong Ouyang, Jun Lu, Georges EL Fakhri, and Jonghye Woo. Domain generalization under conditional and label shifts via variational bayesian inference. *arXiv preprint arXiv:2107.10931*, 2021b.

Paul Michel, Tatsunori Hashimoto, and Graham Neubig. Modeling the second player in distributionally robust optimization. In *International Conference on Learning Representations (ICLR)*, 2021.

K. Muandet, D. Balduzzi, and B. Schölkopf. Domain generalization via invariant feature representation. In *ICML*, 2013.

Hyeonseob Nam, HyunJae Lee, Jongchan Park, Wonjun Yoon, and Donggeun Yoo. Reducing domain gap by reducing style bias. In *CVPR*, 2021.

Lizhen Nie, Mao Ye, Qiang Liu, and Dan Nicolae. Vcnet and functional targeted regularization for learning causal effects of continuous treatments. *ICLR*, 2020.

Sebastian Nowozin, Botond Cseke, and Ryota Tomioka. f-gan: Training generative neural samplers using variational divergence minimization. *Advances in neural information processing systems*, 29, 2016.

Xingchao Peng, Qinxun Bai, Xide Xia, Zijun Huang, Kate Saenko, and Bo Wang. Moment matching for multi-source domain adaptation. In *ICCV*, 2019.

Alexandre Rame, Corentin Dancette, and Matthieu Cord. Fishr: Invariant gradient variances for out-of-distribution generalization. In *International Conference on Machine Learning*, pp. 18347–18377. PMLR, 2022.

Shiori Sagawa, Pang Wei Koh, Tatsunori B Hashimoto, and Percy Liang. Distributionally robust neural networks for group shifts: On the importance of regularization for worst-case generalization. In *International conference on learning representations (ICLR)*, 2020.

Mattia Segu, Alessio Tonioni, and Federico Tombari. Batch normalization embeddings for deep domain generalization. *arXiv preprint arXiv:2011.12672*, 2020.

Yuge Shi, Jeffrey Seely, Philip Torr, Siddharth N, Awni Hannun, Nicolas Usunier, and Gabriel Synnaeve. Gradient matching for domain generalization. In *International Conference on Learning Representations*, 2022. URL <https://openreview.net/forum?id=vDwBW49HmO>.

Aman Sinha, Hongseok Namkoong, Riccardo Volpi, and John Duchi. Certifying some distributional robustness with principled adversarial training. *arXiv preprint arXiv:1710.10571*, 2017.

Matthew Staib and Stefanie Jegelka. Distributionally robust optimization and generalization in kernel methods. *Advances in Neural Information Processing Systems (NeurIPS)*, 2019.

Petar Stojanov, Zijian Li, Mingming Gong, Ruichu Cai, Jaime G. Carbonell, and Kun Zhang. Domain adaptation with invariant representation learning: What transformations to learn? In *NeurIPS*, 2021.

Baochen Sun and Kate Saenko. Deep coral: Correlation alignment for deep domain adaptation. In *ECCV*, 2016.

Yu Sun, Xiaolong Wang, Zhuang Liu, John Miller, Alexei Efros, and Moritz Hardt. Test-time training with self-supervision for generalization under distribution shifts. In *International conference on machine learning*, pp. 9229–9248. PMLR, 2020.

Damien Teney, Seong Joon Oh, and Ehsan Abbasnejad. Id and ood performance are sometimes inversely correlated on real-world datasets. *arXiv preprint arXiv:2209.00613*, 2022.

Antonio Torralba and Alexei A Efros. Unbiased look at dataset bias. In *CVPR*, 2011.

Vladimir Vapnik. *The nature of statistical learning theory*. Springer science & business media, 1999.

Dequan Wang, Evan Shelhamer, Shaoteng Liu, Bruno Olshausen, and Trevor Darrell. Tent: Fully test-time adaptation by entropy minimization. In *ICLR*, 2021.

Shujun Wang, Lequan Yu, Kang Li, Xin Yang, Chi-Wing Fu, and Pheng-Ann Heng. Dofe: Domain-oriented feature embedding for generalizable fundus image segmentation on unseen datasets. *IEEE Transactions on Medical Imaging*, 39(12):4237–4248, 2020.

Shen Yan, Huan Song, Nanxiang Li, Lincan Zou, and Liu Ren. Improve unsupervised domain adaptation with mixup training. *arXiv preprint arXiv:2001.00677*, 2020.

Shiqi Yang, Yaxing Wang, Joost van de Weijer, Luis Herranz, and Shangling Jui. Generalized source-free domain adaptation. In *Proceedings of the IEEE/CVF International Conference on Computer Vision*, pp. 8978–8987, 2021.

Nanyang Ye, Kaican Li, Haoyue Bai, Runpeng Yu, Lanqing Hong, Fengwei Zhou, Zhenguo Li, and Jun Zhu. Ood-bench: Quantifying and understanding two dimensions of out-of-distribution generalization. In *Proceedings of the IEEE/CVF Conference on Computer Vision and Pattern Recognition*, pp. 7947–7958, 2022.

Hanlin Zhang, Yi-Fan Zhang, Weiyang Liu, Adrian Weller, Bernhard Schölkopf, and Eric P Xing. Towards principled disentanglement for domain generalization. In *Proceedings of the IEEE/CVF Conference on Computer Vision and Pattern Recognition*, 2022a.

Kun Zhang, Bernhard Schölkopf, Krikamol Muandet, and Zhikun Wang. Domain adaptation under target and conditional shift. In *International Conference on Machine Learning*, pp. 819–827. PMLR, 2013.

Marvin Zhang, Henrik Marklund, Nikita Dhawan, Abhishek Gupta, Sergey Levine, and Chelsea Finn. Adaptive risk minimization: Learning to adapt to domain shift. *NeurIPS*, 2021a.

Yi-Fan Zhang, Zhang Zhang, Da Li, Zhen Jia, Liang Wang, and Tieniu Tan. Learning domain invariant representations for generalizable person re-identification. *arXiv preprint arXiv:2103.15890*, 2021b.

Yifan Zhang, Bryan Hooi, Lanqing Hong, and Jiashi Feng. Test-agnostic long-tailed recognition by test-time aggregating diverse experts with self-supervision. *arXiv preprint arXiv:2107.09249*, 2021c.

YiFan Zhang, Feng Li, Zhang Zhang, Liang Wang, Dacheng Tao, and Tieniu Tan. Generalizable person re-identification without demographics, 2022b. URL <https://openreview.net/forum?id=VNdFPD5wqjh>.

Han Zhao, Remi Tachet Des Combes, Kun Zhang, and Geoffrey Gordon. On learning invariant representations for domain adaptation. In *ICML*. PMLR, 2019.

Table of Contents

1	Introduction	1
2	Related work	2
3	A Bound by Considering Adaptivity Gap	2
4	Domain-specific Risk Minimization	4
4.1	Domain-specific labeling function	4
4.2	Test-time model selection and adaptation	5
4.2.1	Test-time model selection	5
4.2.2	Test-time retraining	6
5	Experimental Results	6
5.1	Case studies on correlation shift datasets	6
5.2	Results on general OOD benchmarks	7
5.3	Ablation Studies and Analysis	9
6	Concluding Remarks	9
A	Extended Related works	14
B	A Failure Case of Invariant Representation	15
C	Proofs of Theoretical Statements	15
C.1	Derivation and Explanation of the Learning Bound in Eq. 2	15
C.2	Derivation the Learning Bound in Eq. 5	16
C.3	Comparison of the proposed bound to existing bound.	17
C.4	Reformulation of the density ratio.	18
D	Algorithms for Test-time Model Selection Strategies	18
E	Dataset and implementation details	18
E.1	Dataset Details	18
E.2	implementation and hyper-parameter details	19
F	Generalization Results	20
F.1	Detailed Generalization Results	20
F.2	Multi-target domain generalization.	21
G	Additional Analysis	21
G.1	Additional Domain-classifier correlation matrixes	21
G.2	Softing mixed weights	21
G.3	Model complexity	23

A EXTENDED RELATED WORKS

Labeling function shift and multi classifiers. Labeling function shift or correlation shift is not a novel concept and is commonly used in domain adaptation Zhao et al. (2019); Stojanov et al. (2021); Zhang et al. (2013) or domain generalization Ye et al. (2022). There are also some studies on DG that are proposed to tackle this problem. CDANNLi et al. (2018c) considers the scenario where both $P(\bar{X})$ and $P(Y|\bar{X})$ change across domains and proposes to learn a conditional invariant neural network to minimize the discrepancy in $P(X|Y)$ across different domains. Liu et al. (2021b) explores both the correlation and label shifts in DG and aligns the correlation shift via the variational Bayesian inference. The proposed DRM is different from these studies because we want the labeling functions $P(Y|\bar{X})$ more specific to each domain rather than invariant.

B A FAILURE CASE OF INVARIANT REPRESENTATION

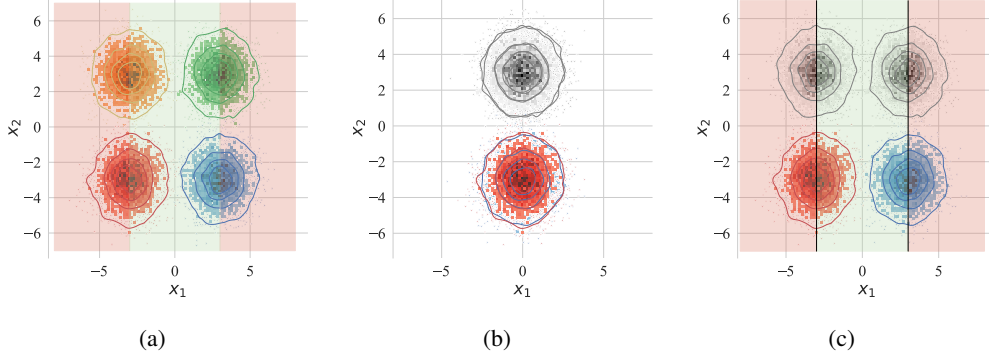


Figure 4: A failure case of invariant representations for domain generalization. (a) Four domains in different colors: orange ($\mu_o = [-3.0, 3.0]$), green ($\mu_g = [3.0, 3.0]$), red ($\mu_r = [-3.0, -3.0]$) and blue ($\mu_b = [3.0, -3.0]$). (b) Invariant representations learnt from domain \mathcal{D}_r and \mathcal{D}_b by feature transformation $g(X) = \mathbb{I}_{x_1 < 0} \cdot (x_1 + 3) + \mathbb{I}_{x_1 > 0} \cdot (x_1 - 3)$. The grey color indicates the transformed target domains. (c) The classification boundary learned by DRM.

DRM can attain 0 source error in the above-mentioned counterexample by using $g(X) = X$ and

$$h_r(X) = \begin{cases} 0 & x_1 \leq -3 \\ 1 & x_1 > -3 \end{cases}, \quad h_b(X) = \begin{cases} 1 & x_1 \leq 3 \\ 0 & x_1 > 3 \end{cases}.$$

Furthermore, the choice of g is not a matter and we can easily generalize it to other cases. For example, given $g(X) = \mathbb{I}_{x_1 < 0} \cdot (x_1 + 3) + \mathbb{I}_{x_1 > 0} \cdot (x_1 - 3)$ for invariant representation. DRM can still attain 0 source error by using

$$h_r(X) = \begin{cases} 0 & x_1 \leq 0 \\ 1 & x_1 > 0 \end{cases}, \quad h_b(X) = \begin{cases} 1 & x_1 \leq 0 \\ 0 & x_1 > 0 \end{cases}$$

Considering the test-time model selection strategy PEM, e.g., in the counterexample, \mathcal{D}_o is more similar to \mathcal{D}_r than to \mathcal{D}_b , hence the entropy when $X \in \mathcal{D}_o$ is classified by h_r is less than the entropy classified by h_b . In this way, Figure 4(c) shows that the learnt classification boundaries can attain 0 test errors on both the unseen target domains \mathcal{D}_o and \mathcal{D}_g .

C PROOFS OF THEORETICAL STATEMENTS

To complete the proofs, we begin by introducing some necessary definitions.

Definition 2. (\mathcal{H} -divergence Ben-David et al. (2006)). *Given two domain distributions $\mathcal{D}_S, \mathcal{D}_T$ over X , and a hypothesis class \mathcal{H} , the \mathcal{H} -divergence between $\mathcal{D}_S, \mathcal{D}_T$ is*

$$d_{\mathcal{H}}(\mathcal{D}_S, \mathcal{D}_T) = 2 \sup_{f \in \mathcal{H}} |\mathbb{E}_{x \sim \mathcal{D}_S}[f(x) = 1] - \mathbb{E}_{x \sim \mathcal{D}_T}[f(x) = 1]|. \quad (7)$$

C.1 DERIVATION AND EXPLANATION OF THE LEARNING BOUND IN EQ. 2

Let $f^* = \arg \min_{\hat{f} \in \mathcal{H}} (\epsilon_{\mathcal{T}}(\hat{f}) + \sum_{i=1}^K \epsilon_i(\hat{f}))$, and let $\lambda_{\mathcal{T}}$ and λ_i be the errors of f^* with respect to $\mathcal{D}_{\mathcal{T}}$ and \mathcal{D}_i respectively. Notice that $\lambda_{\alpha} = \lambda_{\mathcal{T}} + \sum_{i=1}^K \lambda_i$. Similar to Ben-David et al. (2006)

(Theorem 1), we have

$$\begin{aligned}
\epsilon_{\mathcal{T}}(\hat{f}) &\leq \lambda_{\mathcal{T}} + P_{\mathcal{D}_{\mathcal{T}}}[\mathcal{Z}_h \triangle \mathcal{Z}_h^*] \\
&\leq \lambda_{\mathcal{T}} + P_{\mathcal{D}_{\alpha}}[\mathcal{Z}_h \triangle \mathcal{Z}_h^*] + |P_{\mathcal{D}_{\alpha}}[\mathcal{Z}_h \triangle \mathcal{Z}_h^*] - P_{\mathcal{D}_{\mathcal{T}}}[\mathcal{Z}_h \triangle \mathcal{Z}_h^*]| \\
&\leq \lambda_{\mathcal{T}} + P_{\mathcal{D}_{\alpha}}[\mathcal{Z}_h \triangle \mathcal{Z}_h^*] + d_{\mathcal{H}}(\tilde{\mathcal{D}}_{\mathcal{T}}, \tilde{\mathcal{D}}_{\alpha}) \\
&\leq \lambda_{\mathcal{T}} + P_{\mathcal{D}_{\alpha}}[\mathcal{Z}_h \triangle \mathcal{Z}_h^*] + d_{\mathcal{H}}(\tilde{\mathcal{D}}_{\mathcal{T}}^{\alpha}, \tilde{\mathcal{D}}_{\alpha}) + d_{\mathcal{H}}(\tilde{\mathcal{D}}_{\mathcal{T}}, \tilde{\mathcal{D}}_{\mathcal{T}}^{\alpha}) \\
&\leq \lambda_{\mathcal{T}} + \sum_{i=1}^K \lambda_i + \sum_{i=1}^K \alpha_i \epsilon_i(\hat{f}) + d_{\mathcal{H}}(\tilde{\mathcal{D}}_{\mathcal{T}}^{\alpha}, \tilde{\mathcal{D}}_{\alpha}) + d_{\mathcal{H}}(\tilde{\mathcal{D}}_{\mathcal{T}}, \tilde{\mathcal{D}}_{\mathcal{T}}^{\alpha}) \\
&\leq \lambda_{\alpha} + \sum_{i=1}^K \alpha_i \epsilon_i(\hat{f}) + d_{\mathcal{H}}(\tilde{\mathcal{D}}_{\mathcal{T}}^{\alpha}, \tilde{\mathcal{D}}_{\alpha}) + d_{\mathcal{H}}(\tilde{\mathcal{D}}_{\mathcal{T}}, \tilde{\mathcal{D}}_{\mathcal{T}}^{\alpha}),
\end{aligned} \tag{8}$$

The fourth inequality holds because of the triangle inequality. We provide the explanation for our bound in Eq. 8. The second term is the empirical loss for the convex combination of all source domains. The third term corresponds to “To what extent can the convex combination of the source domain approximate the target domain”. The minimization of the third term requires diverse data or strong data augmentation, such that the unseen distribution lies within the convex combination of source domains. For the fourth term, the following equation holds for any two distributions $D'_{\mathcal{T}}, D''_{\mathcal{T}}$, which are the convex combinations of source domains (Albuquerque et al., 2020)

$$d_{\mathcal{H}}[D'_{\mathcal{T}}, D''_{\mathcal{T}}] \leq \sum_{l=1}^K \sum_{k=1}^K \alpha_l \alpha_k d_{\mathcal{H}}[\mathcal{D}_l, \mathcal{D}_k] \tag{9}$$

Such an upper bound will be minimized when $d_{\mathcal{H}}[\mathcal{D}_l, \mathcal{D}_k] = 0, \forall l, k \in \{1, \dots, K\}$. Namely projecting the source domain data into a feature space, where the source domain labels are hard to distinguish.

C.2 DERIVATION THE LEARNING BOUND IN EQ. 5

Proposition 3. Let $\{\mathcal{D}_i, f_i\}_{i=1}^K$ and $\mathcal{D}_{\mathcal{T}}, f_{\mathcal{T}}$ be the empirical distributions and corresponding labeling function. For any hypothesis $\hat{f} \in \mathcal{H}$, given mixed weights $\{\alpha_i\}_{i=1}^K; \sum_{i=1}^K \alpha_i = 1, \alpha_i \geq 0$, we have:

$$\epsilon_{\mathcal{T}}(\hat{f}) \leq \sum_{i=1}^K \left(\mathbb{E}_{X \sim \mathcal{D}_i} \left[\alpha_i \frac{P_{\mathcal{T}}(X)}{P_i(X)} |\hat{f} - f_i| \right] + \alpha_i \mathbb{E}_{\mathcal{D}_{\mathcal{T}}} [|f_i - f_{\mathcal{T}}|] \right)$$

Proof.

$$\begin{aligned}
\epsilon_{\mathcal{T}}(\hat{f}) &= \epsilon_{\mathcal{T}}(\hat{f}, f_{\mathcal{T}}) = \mathbb{E}_{X \sim \mathcal{D}_{\mathcal{T}}} [|\hat{f}(X) - f_{\mathcal{T}}(X)|] \\
&= \sum_{i=1}^K \alpha_i \mathbb{E}_{X \sim \mathcal{D}_{\mathcal{T}}} [|\hat{f}(X) - f_{\mathcal{T}}(X)|] \\
&= \sum_{i=1}^K \alpha_i \left(\mathbb{E}_{X \sim \mathcal{D}_{\mathcal{T}}} [|\hat{f}(X) - f_i(X) + f_i(X) - f_{\mathcal{T}}(X)|] \right) \\
&\leq \sum_{i=1}^K \alpha_i \left(\mathbb{E}_{X \sim \mathcal{D}_{\mathcal{T}}} [|\hat{f}(X) - f_i(X)|] + \mathbb{E}_{X \sim \mathcal{D}_{\mathcal{T}}} [|f_i(X) - f_{\mathcal{T}}(X)|] \right)
\end{aligned}$$

The above proof is based on absolute value inequality. After that, we ignore X in the hypothesis $f(X) \rightarrow f$ for simplicity and apply the change-of-measure trick.

$$\begin{aligned}
\epsilon_{\mathcal{T}}(\hat{f}) &\leq \sum_{i=1}^K \alpha_i \left(\mathbb{E}_{\mathcal{D}_{\mathcal{T}}} [|\hat{f} - f_i|] + \mathbb{E}_{\mathcal{D}_{\mathcal{T}}} [|f_i - f_{\mathcal{T}}|] \right) \\
&= \sum_{i=1}^K \alpha_i \left(\int |\hat{f} - f_i| P_{\mathcal{T}}(X) dX + \mathbb{E}_{\mathcal{D}_{\mathcal{T}}} [|f_i - f_{\mathcal{T}}|] \right) \\
&= \sum_{i=1}^K \alpha_i \left(\int |\hat{f} - f_i| P_i(X) \frac{P_{\mathcal{T}}(X)}{P_i(X)} dX + \mathbb{E}_{\mathcal{D}_{\mathcal{T}}} [|f_i - f_{\mathcal{T}}|] \right) \\
&= \sum_{i=1}^K \left(\mathbb{E}_{X \sim \mathcal{D}_i} \left[\alpha_i \frac{P_{\mathcal{T}}(X)}{P_i(X)} |\hat{f} - f_i| \right] + \alpha_i \mathbb{E}_{\mathcal{D}_{\mathcal{T}}} [|f_i - f_{\mathcal{T}}|] \right),
\end{aligned}$$

which completes our proof. \square

C.3 COMPARISON OF THE PROPOSED BOUND TO EXISTING BOUND.

Before deriving our main result, we first introduce some necessary theorems. For simplicity, given hypothesis $\hat{f}, \hat{f}' \in \mathcal{H}$ and label function f_S for \mathcal{D}_S , denote $\epsilon_S(\hat{f}, \hat{f}') = \mathbb{E}_{\tilde{\mathcal{D}}_S} [|\hat{f} - \hat{f}'|]$ and $\epsilon_S(\hat{f}) = \epsilon_S(\hat{f}, f_S) = \mathbb{E}_{\tilde{\mathcal{D}}_S} [|\hat{f} - f_S|]$, we have

Theorem 1. (Lemma 4.1 and Theorem 4.1 in Albuquerque et al. (2019).) *Given two distribution over image space $\langle \mathcal{D}_S, f_S \rangle, \langle \mathcal{D}_{\mathcal{T}}, f_{\mathcal{T}} \rangle$ and $\hat{f} \in \mathcal{H}$, we have*

$$|\epsilon_S(f_S, f_{\mathcal{T}}) - \epsilon_{\mathcal{T}}(f_S, f_{\mathcal{T}})| \leq d_{\mathcal{H}}(\mathcal{D}_S, \mathcal{D}_{\mathcal{T}}). \quad (10)$$

The error in the target domain can then be bounded by

$$\epsilon_{\mathcal{T}}(\hat{f}) \leq \epsilon_S(\hat{f}) + d_{\mathcal{H}}(\mathcal{D}_S, \mathcal{D}_{\mathcal{T}}) + \min\{\epsilon_S(f_S, f_{\mathcal{T}}), \epsilon_{\mathcal{T}}(f_S, f_{\mathcal{T}})\}, \quad (11)$$

where the result is mainly based on the inequality in Eq. 10.

If only two domains are considered, namely given $\langle \mathcal{D}_S, f_S \rangle, \langle \mathcal{D}_{\mathcal{T}}, f_{\mathcal{T}} \rangle$, recall the derivation of the proposed error bound, we have

$$\begin{aligned}
\epsilon_{\mathcal{T}}(\hat{f}) &\leq \mathbb{E}_{\mathcal{D}_{\mathcal{T}}} [|h - f_S|] + \mathbb{E}_{\mathcal{D}_{\mathcal{T}}} [|f_S - f_{\mathcal{T}}|] \\
&= \epsilon_{\mathcal{T}}(\hat{f}, f_S) + \epsilon_{\mathcal{T}}(f_S, f_{\mathcal{T}}) \\
&= \mathbb{E}_{X \sim \mathcal{D}_S} \left[\frac{P_{\mathcal{T}}(X)}{P_S(X)} |\hat{f} - f_S| \right] + \epsilon_{\mathcal{T}}(f_S, f_{\mathcal{T}})
\end{aligned} \quad (12)$$

Then we will prove that Eq. 12 is upper bounded by Eq. 11. At first, the second line in Eq. 12 is bounded by

$$\begin{aligned}
\epsilon_{\mathcal{T}}(\hat{f}, f_S) + \epsilon_{\mathcal{T}}(f_S, f_{\mathcal{T}}) &\leq \epsilon_S(\hat{f}, f_S) + d_{\mathcal{H}}(\mathcal{D}_S, \mathcal{D}_{\mathcal{T}}) + \epsilon_{\mathcal{T}}(f_S, f_{\mathcal{T}}) \\
&= \epsilon_S(\hat{f}) + \epsilon_{\mathcal{T}}(f_S, f_{\mathcal{T}}) + d_{\mathcal{H}}(\mathcal{D}_S, \mathcal{D}_{\mathcal{T}}).
\end{aligned} \quad (13)$$

Besides, as the density ratio $\frac{P_{\mathcal{T}}(X)}{P_S(X)}$ is intractable and during implementation, this term is set to 1. Namely, the last line of Eq. 12 is approximately equal to

$$\begin{aligned}
&\mathbb{E}_{X \sim \mathcal{D}_S} \left[\frac{P_{\mathcal{T}}(X)}{P_S(X)} |\hat{f} - f_S| \right] + \epsilon_{\mathcal{T}}(f_S, f_{\mathcal{T}}) \\
&= \epsilon_S(\hat{f}) + \epsilon_{\mathcal{T}}(f_S, f_{\mathcal{T}}) \\
&\leq \epsilon_S(\hat{f}) + \epsilon_S(f_S, f_{\mathcal{T}}) + d_{\mathcal{H}}(\mathcal{D}_S, \mathcal{D}_{\mathcal{T}})
\end{aligned} \quad (14)$$

Combining Eq. 13 and Eq. 14 we can get the error bound in Eq. 12 is upper bounded by

$$\epsilon_S(\hat{f}) + d_{\mathcal{H}}(\mathcal{D}_S, \mathcal{D}_{\mathcal{T}}) + \min\{\epsilon_S(f_S, f_{\mathcal{T}}), \epsilon_{\mathcal{T}}(f_S, f_{\mathcal{T}})\}, \quad (15)$$

which completes our proof.

C.4 REFORMULATION OF THE DENSITY RATIO.

Although estimating $P_{\mathcal{T}}(x)/P_i(x)$ directly is intractable, we can add constraints to the unseen target domain and get applicable formulations, which is just what distributionally robust optimization (DRO) (Ben-Tal et al., 2009) does. Specifically, if we restrict the target domain within a f -divergence ball (such as Kullback-Leibler divergence) from the training distribution, which is also known as KL-DRO (Hu & Hong, 2013), then the density ratio will be converted to a reweighting term $e^{\ell/\tau^*}/\mathbb{E}[e^{\ell/\tau^*}]$ used for training, where ℓ indicates the classification error incurred by (x, y) and τ^* is a hyperparameter. Namely the reweighting term is actually an approximate estimation of the density ratio. Existing methods (Liu et al., 2021a; Zhang et al., 2022b; Sagawa et al., 2020) use similar reweighting terms and our error bound provides a theoretical explanation for why they work well on DG.

In this subsection, we first introduce some important definitions of the distributionally robust optimization (DRO) framework Ben-Tal et al. (2009) and then reformulate the density ratio under some necessary assumptions. In DRO, the worst-case expected risk over a predefined family of distributions \mathcal{Q} (termed *uncertainty set*) is used to replace the expected risk on the unseen target distribution \mathcal{T} in ERM. Therefore, the objective is as follows,

$$\min_{\theta \in \Theta} \max_{q \in \mathcal{Q}} \mathbb{E}_{(x,y) \in q} [\ell(x, y; \theta)]. \quad (16)$$

Specifically, the uncertainty set \mathcal{Q} encodes the possible test distributions that we want our model to perform well on. If \mathcal{Q} contains \mathcal{T} , the DRO object can upper bound the expected risk under \mathcal{T} .

The construction of uncertainty set \mathcal{Q} is of vital importance. Here we reformulate the density ratio based on the KL-divergence ball constraint and other choices (e.g., using moment constraint Delage & Ye (2010), f -divergence Michel et al. (2021), Wasserstein/MMD ball Sinha et al. (2017); Staib & Jegelka (2019)) will lead to different reweighting methods. Given the KL upper bound (radius) η , denote the empirical distribution \mathcal{P} , we have the uncertainty set $\mathcal{Q} = \{Q : \text{KL}(Q||\mathcal{P}) \leq \eta\}$. The min-max problem in Eq. 16 can then be reformulated as

$$\min_{\theta \in \Theta} \max_{Q: \text{KL}(Q||\mathcal{P}) \leq \eta} \mathbb{E}_{(x,y) \in Q} [\ell(x, y; \theta)]. \quad (17)$$

Then we have the following theorem, which derives the optimal density ratio and converts the original problem to a reweighting version.

Theorem 2. (Modified from Section 2 in Hu & Hong (2013)) Assume the model family $\theta \in \Theta$ and \mathcal{Q} to be convex and compact. The loss ℓ is continuous and convex for all $x \in \mathcal{X}, y \in \mathcal{Y}$. Suppose empirical distribution \mathcal{P} has density $p(x, y)$. Then the inner maximum of Eq. 17 has a closed-form solution

$$q^*(x, y) = \frac{p(x, y) e^{\ell(x, y; \theta)/\tau^*}}{\mathbb{E}_{\mathcal{P}} [e^{\ell(x, y; \theta)/\tau^*}]}, \quad (18)$$

where τ^* satisfies $\mathbb{E}_{\mathcal{P}} \left[\frac{e^{\ell(x, y; \theta)/\tau^*}}{\mathbb{E}_{\mathcal{P}} [e^{\ell(x, y; \theta)/\tau^*}]} \left(\frac{\ell(x, y; \theta)}{\tau^*} - \log \mathbb{E}_{\mathcal{P}} [e^{\ell(x, y; \theta)/\tau^*}] \right) \right] = \eta$ and $q^*(x, y)$ is the optimal density of Q . The min-max problem in Eq. 17 is then equivalent to

$$\min_{\theta \in \Theta, \tau > 0} \tau \log \mathbb{E}_{\mathcal{P}} \left[e^{\ell(x, y; \theta)/\tau} \right] + \eta \tau. \quad (19)$$

D ALGORITHMS FOR TEST-TIME MODEL SELECTION STRATEGIES

E DATASET AND IMPLEMENTATION DETAILS

E.1 DATASET DETAILS

Colored MNIST Arjovsky et al. (2019) consists of digits in MNIST with different colors (either blue or red). The label is a noisy function of the digit and color. First, a preliminary label \bar{y} is assigned to images based on their digits, $\bar{y} = 0$ for digits 0-4 and $\bar{y} = 1$ for digits 5-9. The final label is obtained by flipping \bar{y} with probability 0.25. The color signal z of each sample is obtained by flipping

Algorithm 1: Cosine Similarity Measurement (CSM).

Input: training data $\{\mathcal{D}_i\}_{i=1}^K$, test data \mathcal{D}_T , batch size N , learning rate η , training iterations T .
Initial: Classifiers $\{h_i\}_{i=1}^K$ with parameter $\{\theta_i^h\}_{i=1}^K$, encoder g with parameter θ^g .
//During Training
for $t = 1, \dots, T$ **do**
 $\left| \begin{array}{l} \{(x_i^k, y_i^k, d_k)_{i=1}^N \sim \mathcal{D}_i\}_{k=1}^K \quad // Data sampling, (data, label, domain label) \\ \mathcal{L} = \sum_{k=1}^K \sum_{i=1}^N \ell(x_i^k, y_i^k; \theta^{g,t-1}, \theta_i^{h,t-1}) \quad // Calculate the empirical loss \\ \theta^{g,t} \leftarrow \text{SGD}(\mathcal{L}, \theta^{g,t-1}, \eta); \{\theta_i^{h,t} \leftarrow \text{SGD}(\mathcal{L}, \theta_i^{h,t-1}, \eta)\}_{i=1}^K \quad // Update parameters \end{array} \right.$
end
//During Test
Calculate domain representations. $\{z_i = \frac{1}{|\mathcal{D}_i|} \sum_{x \in \mathcal{D}_i} g(x)\}_{i=1}^K$
for $x \in \mathcal{D}_T$ **do**
 $\left| \begin{array}{l} \{H_i = \text{cosine}_{\text{similarity}}(g(x), z_i)\}_{i=1}^K \quad // Calculate similarities. \\ i^* = \arg \max \{H_i\}_{i=1}^K \quad // Similarity Maximization. \\ y_t = \arg \max \bar{y}^{i^*} \text{ if not ensembling else } \arg \max \sum_{k=1}^K \bar{y}_k \frac{H_k^\gamma}{\sum_{i=1}^K H_i^\gamma} \quad // Result. \end{array} \right.$
end

Algorithm 2: Prediction Entropy Measurement (PEM).

Input: training data $\{\mathcal{D}_i\}_{i=1}^K$, test data \mathcal{D}_T , batch size N , learning rate η , training iterations T .
Initial: Classifiers $\{h_i\}_{i=1}^K$ with parameter $\{\theta_i^h\}_{i=1}^K$, encoder g with parameter θ^g .
//Training Process is the same as Algorithm 1
//During Test
for $x \in \mathcal{D}_T$ **do**
 $\left| \begin{array}{l} \bar{y}^i := [y_1^i, \dots, y_c^i] = h_i \circ g(x) \quad // Make prediction by every classifier \\ \{H_k = -\sum_{i=1}^c \frac{y_i^k}{\sum_{j=1}^c y_j^k} \log \frac{y_i^k}{\sum_{j=1}^c y_j^k}\}_{k=1}^K \quad // Calculate the prediction entropy. \\ i^* = \arg \min \{H_i\}_{i=1}^K \quad // Prediction Entropy Minimization. \\ y_t = \arg \max \bar{y}^{i^*} \text{ if not ensembling else } \arg \max \sum_{k=1}^K \bar{y}_k \frac{H_k^{-\gamma}}{\sum_{i=1}^K H_i^{-\gamma}} \quad // Result. \\ // The weighting term here is $H_i^{-\gamma}$ not H_i^γ in the other two strategies because the result with small entropy should be assigned a large weight. \end{array} \right.$
end

y with probability p^d , where p^d is $\{0.2, 0.1, 0.9\}$ for three different domains. Finally, images with $z = 1$ will be colored red and $z = 0$ will be colored blue. This dataset contains 70,000 examples of dimension $(2, 28, 28)$ and 2 classes.

Rotated MNIST Ghifary et al. (2015) consists of 10,000 digits in MNIST with different rotated angles where domain is determined by the degrees $d \in \{0, 15, 30, 45, 60, 75\}$.

PACS Li et al. (2017) includes 9, 991 images with 7 classes $y \in \{ \text{dog, elephant, giraffe, guitar, horse, house, person} \}$ from 4 domains $d \in \{\text{art, cartoons, photos, sketches}\}$.

VLCS Torralba & Efros (2011) is composed of 10,729 images, 5 classes $y \in \{ \text{bird, car, chair, dog, person} \}$ from domains $d \in \{\text{Caltech101, LabelMe, SUN09, VOC2007}\}$.

DomainNet Peng et al. (2019) has six domains $d \in \{\text{clipart, infograph, painting, quickdraw, real, sketch}\}$. This dataset contains 586, 575 examples of size $(3, 224, 224)$ and 345 classes.

E.2 IMPLEMENTATION AND HYPER-PARAMETER DETAILS

Hyperparameter search. Following the experimental settings in (Gulrajani & Lopez-Paz, 2021), we conduct a random search of 20 trials over the hyperparameter distribution for each algorithm and test domain. Specifically, we split the data from each domain into 80% and 20% proportions, where the

Table 9: Domain generalization accuracies (%) on Colored MNIST.

Algorithm	+90%	+80%	-90%	Avg
ERM Vapnik (1999)	71.8 ± 0.4	72.9 ± 0.1	28.7 ± 0.5	57.8
IRM Arjovsky et al. (2019)	72.0 ± 0.1	72.5 ± 0.3	58.5 ± 3.3	67.7
GDRO Sagawa et al. (2020)	73.5 ± 0.3	73.0 ± 0.3	36.8 ± 2.8	61.1
Mixup Yan et al. (2020)	72.5 ± 0.2	73.9 ± 0.4	28.6 ± 0.2	58.4
MLDG Li et al. (2018a)	71.9 ± 0.3	73.5 ± 0.2	29.1 ± 0.9	58.2
CORAL Sun & Saenko (2016)	71.1 ± 0.2	73.4 ± 0.2	31.1 ± 1.6	58.6
MMD Li et al. (2018b)	69.0 ± 2.3	70.4 ± 1.6	50.6 ± 0.2	63.3
DANN Ganin et al. (2016)	72.4 ± 0.5	73.9 ± 0.5	24.9 ± 2.7	57.0
CDANN Li et al. (2018c)	71.8 ± 0.5	72.9 ± 0.1	33.8 ± 6.4	59.5
MTL Blanchard et al. (2021)	71.2 ± 0.2	73.5 ± 0.2	28.0 ± 0.6	57.6
SagNet Nam et al. (2021)	72.1 ± 0.3	73.2 ± 0.3	29.4 ± 0.5	58.2
ARM Zhang et al. (2021a)	84.9 ± 0.9	76.8 ± 0.6	27.9 ± 2.1	63.2
VREx Krueger et al. (2021)	72.8 ± 0.3	73.0 ± 0.3	55.2 ± 4.0	67.0
RSC Huang et al. (2020)	72.0 ± 0.1	73.2 ± 0.1	30.2 ± 1.6	58.5
DRM	86.7 ± 2.4	80.6 ± 0.2	43.1 ± 7.5	70.1
DRM + CORAL	85.3 ± 2.3	80.7 ± 0.2	47.2 ± 3.6	71.1

larger split is used for training and evaluation, and the smaller ones are used for select hyperparameters. We repeat the entire experiment twice using different seeds to reduce the randomness. Finally, we report the mean over these repetitions as well as their estimated standard error. We observe that the proposed DRM does not converge within $5k$ iterations on the DomainNet dataset and we thus train it with an extra $5k$ iterations.

Implementation details. During training, we use the average of all classifiers’ losses as the training loss. To further enlarge the hypothesis space, we can simply add an additional prediction head that is trained by all data samples, namely, we have total of $K + 1$ prediction heads in the test phase, such a simple trick is optional and can bring performance gains on some of our benchmarks.

Model selection. The model selection in domain generalization is intrinsically a learning problem, and we use test-domain validation, one of the three selection methods in (Gulrajani & Lopez-Paz, 2021). This strategy is an oracle-selection one since we choose the model maximizing the accuracy on a validation set that follows the distribution of the test domain.

Model architectures. Following (Gulrajani & Lopez-Paz, 2021), we use as encoders ConvNet for RotatedMNIST (detailed in Appdendix D.1 in (Gulrajani & Lopez-Paz, 2021)) and ResNet-50 for the remaining datasets.

F GENERALIZATION RESULTS

F.1 DETAILED GENERALIZATION RESULTS

Table. 9 shows the generalization performance on the ColoredMNIST of all baseline algorithms. No existing algorithm performs better than IRM, however, the proposed DRM and its variants (incorporated with CORAL) beats these algorithms by a large margin. Generalization results on the Rotated MNIST (Table 12) show that the proposed DRM and its variants perform much better than baselines on challenging domains (domain $d = 0$ and domain $d = 5$) and then attain a better average generalization accuracy. For large benchmarks VLCS, PACS, and DomainNet, generalization results are shown in Table 13, Table 13, and Table 12 respectively. We observe that DRM outperforms existing algorithms on all these benchmarks, however, because CORAL performs not better than ERM in these benchmarks, incorporating CORAL with DRM is sometimes harmful.

Table 10: Generalization performance on multiple unseen target domains.

Method	Rotated MNIST						Avg
	Target domains $\{0, 30, 60\}$			Target domains $\{15, 45, 75\}$			
0	30	60	15	45	75		
ERM	96.0 \pm 0.3	98.8 \pm 0.4	98.7 \pm 0.1	98.8 \pm 0.3	99.1\pm0.1	96.7 \pm 0.3	98.0
IRM	80.9 \pm 3.2	94.7 \pm 0.9	94.3 \pm 1.3	94.3 \pm 0.8	95.5 \pm 0.5	91.1 \pm 3.1	91.8
DRM	97.1\pm0.2	98.8\pm0.2	98.9\pm0.3	98.8\pm0.1	98.8 \pm 0.0	98.1\pm0.7	98.4

Table 11: In-distribution performance on Rotated MNIST and DomainNet.

Method	Rotated MNIST						Avg
	0	15	30	45	60	75	
ERM	99.1\pm0.2	98.8 \pm 0.5	99.0 \pm 0.1	99.1\pm0.2	99.0 \pm 0.2	98.9 \pm 0.4	99.0
IRM	92.9 \pm 1.8	92.6 \pm 2.5	94.7 \pm 1.0	89.9 \pm 1.5	92.1 \pm 2.2	94.9 \pm 1.5	92.9
DRM	99.0 \pm 0.2	99.0\pm0.3	99.0\pm0.3	99.0 \pm 0.2	99.1\pm0.2	99.0\pm0.2	99.0

Method	DomainNet						Avg
	clip	info	paint	quick	real	sketch	
ERM	50.4\pm11.4	58.3 \pm 6.2	53.4\pm12.6	54.6 \pm 12.7	50.8\pm11.0	51.9 \pm 12.6	53.2
IRM	33.4 \pm 4.1	53.2 \pm 1.4	34.0 \pm 4.1	35.1 \pm 3.4	33.0 \pm 3.8	31.5 \pm 3.1	36.7
DRM	50.1 \pm 14.3	58.3\pm10.4	52.5 \pm 14.7	58.1\pm10.3	50.2 \pm 13.2	52.1\pm11.5	53.6

F.2 MULTI-TARGET DOMAIN GENERALIZATION.

IRM Arjovsky et al. (2019) introduces specific conditions for an upper bound on the number of training environments required such that an invariant optimal model can be obtained, which stresses the importance of several training environments. In this paper, we reduce the training environments on the Rotated MNIST from five to three. As shown in Table 10, as the number of training environment decreases, the performance of IRM fall sharply (e.g., the averaged accuracy from 97.5% to 91.8%), and the performance on the most challenging domains $d = \{0, 5\}$ decline the most (94.9% \rightarrow 80.9% and 95.2% \rightarrow 91.1%). In contrast, both ERM and DRM retain high generalization performances while DRM outperforms ERM on domains $d = \{0, 5\}$.

G ADDITIONAL ANALYSIS

G.1 ADDITIONAL DOMAIN-CLASSIFIER CORRELATION MATRIXES

Figure 7 shows all Domain-classifier correlation matrixes on the Rotated MNIST, PACS, and VLCS datasets with different domains as the unseen target domain. The three characteristics mentioned in Sec. 5.3 still hold on to these matrixes. Besides, these Domain-classifier correlation matrixes reflect some dataset properties that cannot be observed by humans directly. As shown in Figure 5, domains in the VLCS dataset do not show significant visual differences, at least not as obvious as the rotation angle on Rotated MNIST or image style on PACS. However, the correlation matrixes attained by DRM still have distinct prediction entropy on different domain-classifier pairs.

G.2 SOFTING MIXED WEIGHTS

Figure 6 shows ablation experiments of hyper-parameter γ on three benchmarks. Different benchmarks show different preferences on γ . For easy benchmarks Rotated MNIST and Colored MNIST, softening mixed weights is needless. The reason behind this phenomenon can be found in Figure 2(d), the optimal classifier for target domain 0 of Rotated MNIST is exactly the classifier 1 and the prediction entropies will increase as the rotation angle increases. Hence, selecting the most approximate classifier based on the minimum entropy selection strategy is enough to attain superior generalization results. However, prediction entropies on other larger benchmarks, e.g., VLCS, are not so regular as on the Rotated MNIST. On realistic benchmarks, a mixing of classifiers can bring some improvements.

Table 12: Domain generalization accuracies (%) on Rotated MNIST and DomainNet.

Algorithm	Rotated MNIST						
	0	15	30	45	60	75	Avg
ERM Vapnik (1999)	95.3 \pm 0.2	98.7 \pm 0.1	98.9 \pm 0.1	98.7 \pm 0.2	98.9 \pm 0.0	96.2 \pm 0.2	97.8
IRM Arjovsky et al. (2019)	94.9 \pm 0.6	98.7 \pm 0.2	98.6 \pm 0.1	98.6 \pm 0.2	98.7 \pm 0.1	95.2 \pm 0.3	97.5
GDRO Sagawa et al. (2020)	95.9 \pm 0.1	99.0 \pm 0.1	98.9 \pm 0.1	98.8 \pm 0.1	98.6 \pm 0.1	96.3 \pm 0.4	97.9
Mixup Yan et al. (2020)	95.8 \pm 0.3	98.7 \pm 0.0	99.0 \pm 0.1	98.8 \pm 0.1	98.8 \pm 0.1	96.6 \pm 0.2	98.0
MLDG Li et al. (2018a)	95.7 \pm 0.2	98.9 \pm 0.1	98.8 \pm 0.1	98.9 \pm 0.1	98.6 \pm 0.1	95.8 \pm 0.4	97.8
CORAL Sun & Saenko (2016)	96.2 \pm 0.2	98.8 \pm 0.1	98.8 \pm 0.1	98.8 \pm 0.1	98.9 \pm 0.1	96.4 \pm 0.2	98.0
MMD Li et al. (2018b)	96.1 \pm 0.2	98.9 \pm 0.0	99.0 \pm 0.0	98.8 \pm 0.0	98.9 \pm 0.0	96.4 \pm 0.2	98.0
DANN Ganin et al. (2016)	95.9 \pm 0.1	98.9 \pm 0.1	98.6 \pm 0.2	98.7 \pm 0.1	98.9 \pm 0.0	96.3 \pm 0.3	97.9
CDANN Li et al. (2018c)	95.9 \pm 0.2	98.8 \pm 0.0	98.7 \pm 0.1	98.9 \pm 0.1	98.8 \pm 0.1	96.1 \pm 0.3	97.9
MTL Blanchard et al. (2021)	96.1 \pm 0.2	98.9 \pm 0.0	99.0 \pm 0.0	98.7 \pm 0.1	99.0 \pm 0.0	95.8 \pm 0.3	97.9
SagNet Nam et al. (2021)	95.9 \pm 0.1	99.0 \pm 0.1	98.9 \pm 0.1	98.6 \pm 0.1	98.8 \pm 0.1	96.3 \pm 0.1	97.9
ARM Zhang et al. (2021a)	95.9 \pm 0.4	99.0 \pm 0.1	98.8 \pm 0.1	98.9 \pm 0.1	99.1 \pm 0.1	96.7 \pm 0.2	98.1
VREx Krueger et al. (2021)	95.5 \pm 0.2	99.0 \pm 0.0	98.7 \pm 0.2	98.8 \pm 0.1	98.8 \pm 0.0	96.4 \pm 0.0	97.9
RSC Huang et al. (2020)	95.4 \pm 0.1	98.6 \pm 0.1	98.6 \pm 0.1	98.9 \pm 0.0	98.8 \pm 0.1	95.4 \pm 0.3	97.6
DRM	96.4 \pm 0.2	98.4 \pm 0.0	98.9 \pm 0.2	99.0 \pm 0.2	98.9 \pm 0.2	96.8 \pm 0.2	98.1
DRM + CORAL	96.9 \pm 0.1	98.9 \pm 0.2	98.9 \pm 0.4	99.0 \pm 0.1	98.9 \pm 0.2	97.3 \pm 0.3	98.3

Algorithm	DomainNet						Avg
	clip	info	paint	quick	real	sketch	
ERM Vapnik (1999)	58.1 \pm 0.3	18.8 \pm 0.3	46.7 \pm 0.3	12.2 \pm 0.4	59.6 \pm 0.1	49.8 \pm 0.4	40.9
IRM Arjovsky et al. (2019)	48.5 \pm 2.8	15.0 \pm 1.5	38.3 \pm 4.3	10.9 \pm 0.5	48.2 \pm 5.2	42.3 \pm 3.1	33.9
GDRO Sagawa et al. (2020)	47.2 \pm 0.5	17.5 \pm 0.4	33.8 \pm 0.5	9.3 \pm 0.3	51.6 \pm 0.4	40.1 \pm 0.6	33.3
Mixup Yan et al. (2020)	55.7 \pm 0.3	18.5 \pm 0.5	44.3 \pm 0.5	12.5 \pm 0.4	55.8 \pm 0.3	48.2 \pm 0.5	39.2
MLDG Li et al. (2018a)	59.1 \pm 0.2	19.1 \pm 0.3	45.8 \pm 0.7	13.4 \pm 0.3	59.6 \pm 0.2	50.2 \pm 0.4	41.2
CORAL Sun & Saenko (2016)	59.2 \pm 0.1	19.7 \pm 0.2	46.6 \pm 0.3	13.4 \pm 0.4	59.8 \pm 0.2	50.1 \pm 0.6	41.5
MMD Li et al. (2018b)	32.1 \pm 13.3	11.0 \pm 4.6	26.8 \pm 11.3	8.7 \pm 2.1	32.7 \pm 13.8	28.9 \pm 11.9	23.4
DANN Ganin et al. (2016)	53.1 \pm 0.2	18.3 \pm 0.1	44.2 \pm 0.7	11.8 \pm 0.1	55.5 \pm 0.4	46.8 \pm 0.6	38.3
CDANN Li et al. (2018c)	54.6 \pm 0.4	17.3 \pm 0.1	43.7 \pm 0.9	12.1 \pm 0.7	56.2 \pm 0.4	45.9 \pm 0.5	38.3
MTL Blanchard et al. (2021)	57.9 \pm 0.5	18.5 \pm 0.4	46.0 \pm 0.1	12.5 \pm 0.1	59.5 \pm 0.3	49.2 \pm 0.1	40.6
SagNet Nam et al. (2021)	57.7 \pm 0.3	19.0 \pm 0.2	45.3 \pm 0.3	12.7 \pm 0.5	58.1 \pm 0.5	48.8 \pm 0.2	40.3
ARM Zhang et al. (2021a)	49.7 \pm 0.3	16.3 \pm 0.5	40.9 \pm 1.1	9.4 \pm 0.1	53.4 \pm 0.4	43.5 \pm 0.4	35.5
VREx Krueger et al. (2021)	47.3 \pm 3.5	16.0 \pm 1.5	35.8 \pm 4.6	10.9 \pm 0.3	49.6 \pm 4.9	42.0 \pm 3.0	33.6
RSC Huang et al. (2020)	55.0 \pm 1.2	18.3 \pm 0.5	44.4 \pm 0.6	12.2 \pm 0.2	55.7 \pm 0.7	47.8 \pm 0.9	38.9
DRM	59.2 \pm 0.2	20.8 \pm 0.3	47.2 \pm 0.1	15.2 \pm 0.2	60.9 \pm 0.6	50.8 \pm 0.5	42.4
DRM + CORAL	59.3 \pm 0.1	22.0 \pm 0.9	48.0 \pm 0.9	15.1 \pm 0.2	61.0 \pm 0.0	50.9 \pm 0.1	42.7

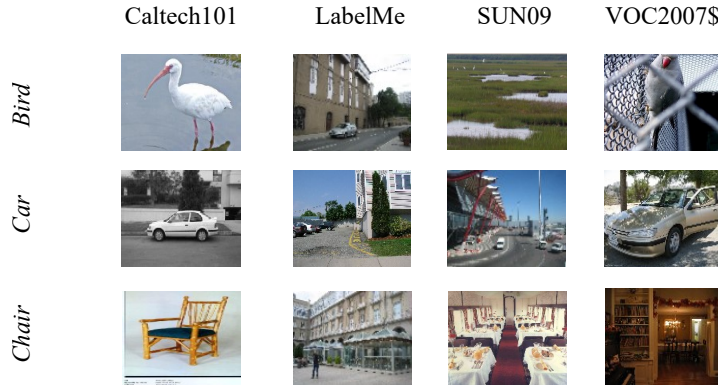


Figure 5: Samples on VLCS.

Besides, normalization, which is a method to reduce classification confidence⁵, is also needless for semi-synthetic datasets (Rotated MNIST and Colored MNIST) and valuable for realistic benchmarks.

⁵Given two classification results from 2 classifiers [2.1, 0.4, 0.5], [0.3, 0.6, 0.1] and assume the weights are all 1. The result is [2.4, 1.0, 0.6] with normalization and [1.0, 0.73, 0.27] without normalization. The former is more confident than the latter.

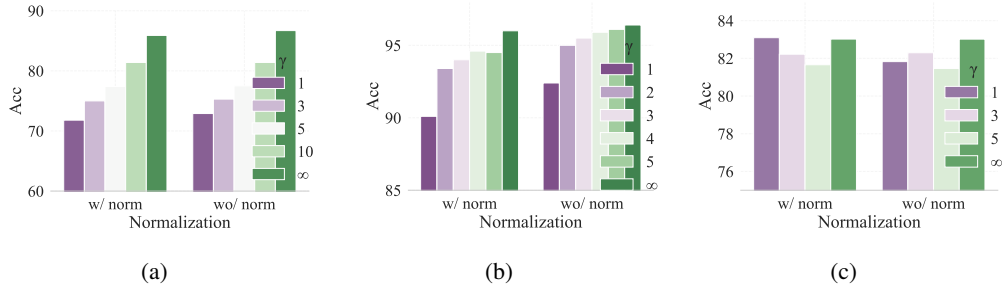


Figure 6: Different mixing weights on the (a) Colored MNIST (target domain $d = 2$) (b) Rotated MNIST (target domain $d = 0$), and (c) PACS datasets (target domain $d = 3$). Given a classification vector $\bar{y} = [y_1, y_2, \dots, y_c]$, c is the number of classes, performing normalization means that let $y_i = y_i / \sum_{j=1}^c y_j$ before mixing.

G.3 MODEL COMPLEXITY

As the number of domains/classes increases or the feature dimension increases, the training time of DRM will increase accordingly, however, DRM is always comparable to ERM and much faster than Fish and ARM (Table 14). For model parameters, since all classifiers in our implementation are just a linear layer, the total parameters of DRM is similar to ERM and much less than existing methods such as CDANN and ARM.

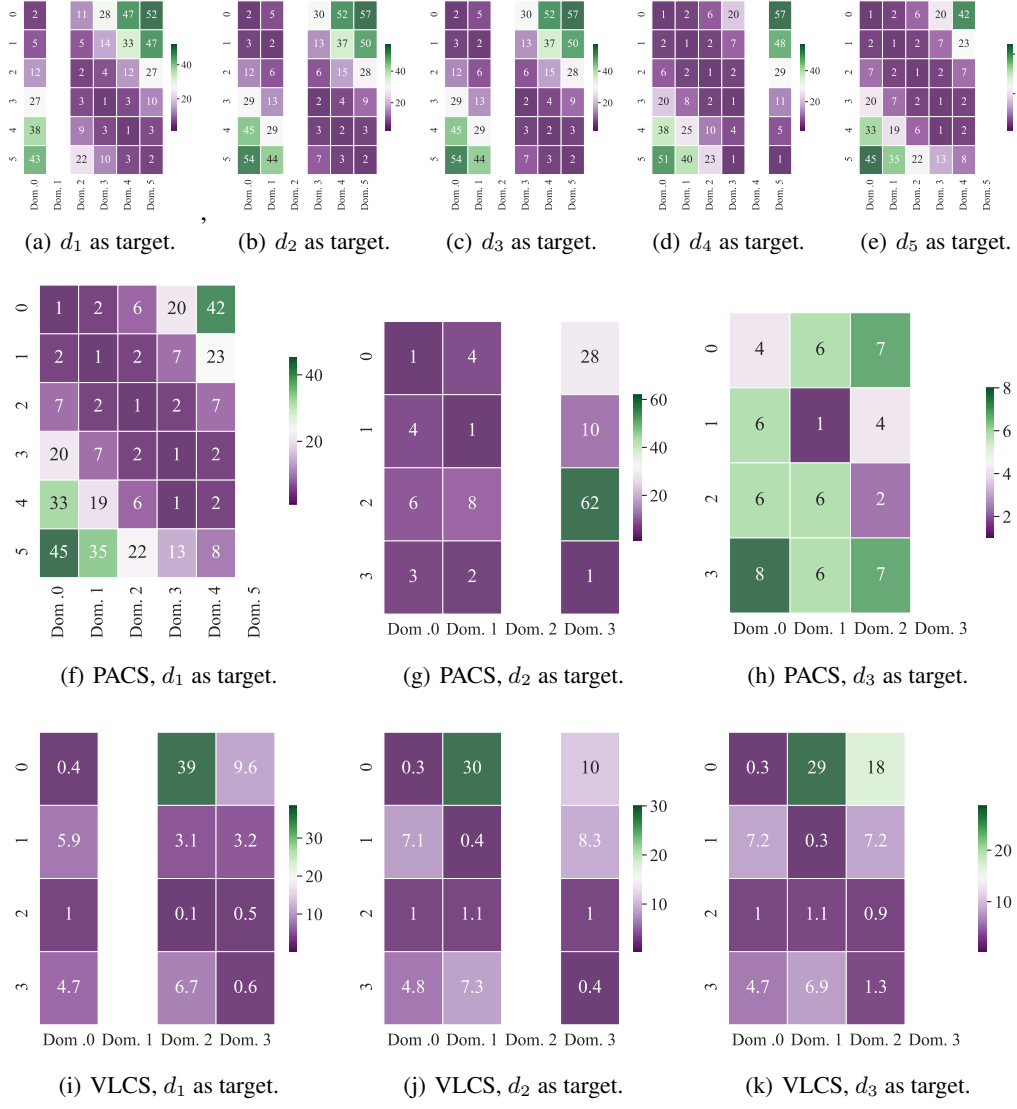


Figure 7: Domain-classifier correlation matrixes on (a,b,c,d,e) Rotated MNIST, (f,g,h) PACS, and (i,j,k) VLCS datasets.

Table 13: Domain generalization accuracies (%) on VLCS and PACS.

Algorithm	VLCS					Avg
	C	L	S	V		
ERM Vapnik (1999)	97.6 \pm 0.3	67.9 \pm 0.7	70.9 \pm 0.2	74.0 \pm 0.6	77.6	
IRM Arjovsky et al. (2019)	97.3 \pm 0.2	66.7 \pm 0.1	71.0 \pm 2.3	72.8 \pm 0.4	76.9	
GDRO Sagawa et al. (2020)	97.7 \pm 0.2	65.9 \pm 0.2	72.8 \pm 0.8	73.4 \pm 1.3	77.4	
Mixup Yan et al. (2020)	97.8 \pm 0.4	67.2 \pm 0.4	71.5 \pm 0.2	75.7 \pm 0.6	78.1	
MLDG Li et al. (2018a)	97.1 \pm 0.5	66.6 \pm 0.5	71.5 \pm 0.1	75.0 \pm 0.9	77.5	
CORAL Sun & Saenko (2016)	97.3 \pm 0.2	67.5 \pm 0.6	71.6 \pm 0.6	74.5 \pm 0.0	77.7	
MMD Li et al. (2018b)	98.8 \pm 0.0	66.4 \pm 0.4	70.8 \pm 0.5	75.6 \pm 0.4	77.9	
DANN Ganin et al. (2016)	99.0 \pm 0.2	66.3 \pm 1.2	73.4 \pm 1.4	80.1 \pm 0.5	79.7	
CDANN Li et al. (2018c)	98.2 \pm 0.1	68.8 \pm 0.5	74.3 \pm 0.6	78.1 \pm 0.5	79.9	
MTL Blanchard et al. (2021)	97.9 \pm 0.7	66.1 \pm 0.7	72.0 \pm 0.4	74.9 \pm 1.1	77.7	
SagNet Nam et al. (2021)	97.4 \pm 0.3	66.4 \pm 0.4	71.6 \pm 0.1	75.0 \pm 0.8	77.6	
ARM Zhang et al. (2021a)	97.6 \pm 0.6	66.5 \pm 0.3	72.7 \pm 0.6	74.4 \pm 0.7	77.8	
VREx Krueger et al. (2021)	98.4 \pm 0.2	66.4 \pm 0.7	72.8 \pm 0.1	75.0 \pm 1.4	78.1	
RSC Huang et al. (2020)	98.0 \pm 0.4	67.2 \pm 0.3	70.3 \pm 1.3	75.6 \pm 0.4	77.8	
DRM	97.5 \pm 0.2	71.8 \pm 1.2	76.6 \pm 0.3	76.4 \pm 1.0	80.5	
DRM + CORAL	97.1 \pm 1.3	72.3 \pm 1.1	73.6 \pm 3.1	74.2 \pm 0.4	79.5	

Algorithm	PACS					Avg
	A	C	P	S		
ERM Vapnik (1999)	86.5 \pm 1.0	81.3 \pm 0.6	96.2 \pm 0.3	82.7 \pm 1.1	86.7	
IRM Arjovsky et al. (2019)	84.2 \pm 0.9	79.7 \pm 1.5	95.9 \pm 0.4	78.3 \pm 2.1	84.5	
GDRO Sagawa et al. (2020)	87.5 \pm 0.5	82.9 \pm 0.6	97.1 \pm 0.3	81.1 \pm 1.2	87.1	
Mixup Yan et al. (2020)	87.5 \pm 0.4	81.6 \pm 0.7	97.4 \pm 0.2	80.8 \pm 0.9	86.8	
MLDG Li et al. (2018a)	87.0 \pm 1.2	82.5 \pm 0.9	96.7 \pm 0.3	81.2 \pm 0.6	86.8	
CORAL Sun & Saenko (2016)	86.6 \pm 0.8	81.8 \pm 0.9	97.1 \pm 0.5	82.7 \pm 0.6	87.1	
MMD Li et al. (2018b)	88.1 \pm 0.8	82.6 \pm 0.7	97.1 \pm 0.5	81.2 \pm 1.2	87.2	
DANN Ganin et al. (2016)	87.0 \pm 0.4	80.3 \pm 0.6	96.8 \pm 0.3	76.9 \pm 1.1	85.2	
CDANN Li et al. (2018c)	87.7 \pm 0.6	80.7 \pm 1.2	97.3 \pm 0.4	77.6 \pm 1.5	85.8	
MTL Blanchard et al. (2021)	87.0 \pm 0.2	82.7 \pm 0.8	96.5 \pm 0.7	80.5 \pm 0.8	86.7	
SagNet Nam et al. (2021)	87.4 \pm 0.5	81.2 \pm 1.2	96.3 \pm 0.8	80.7 \pm 1.1	86.4	
ARM Zhang et al. (2021a)	85.0 \pm 1.2	81.4 \pm 0.2	95.9 \pm 0.3	80.9 \pm 0.5	85.8	
VREx Krueger et al. (2021)	87.8 \pm 1.2	81.8 \pm 0.7	97.4 \pm 0.2	82.1 \pm 0.7	87.2	
RSC Huang et al. (2020)	86.0 \pm 0.7	81.8 \pm 0.9	96.8 \pm 0.7	80.4 \pm 0.5	86.2	
DRM	87.4 \pm 2.9	83.5 \pm 0.8	96.0 \pm 0.5	83.0 \pm 0.7	87.5	
DRM + CORAL	87.7 \pm 1.7	81.7 \pm 0.5	97.1 \pm 0.2	83.1 \pm 1.2	87.4	

Table 14: Comparisons of different methods on the number of parameters and training time.

Method	Colored MNIST		Rotated MNIST		PACS	
	Time (sec)	# Params (M)	Time (sec)	# Params (M)	Time (sec)	# Params (M)
ERM	71.02	0.3542	168.32	0.3546	2,717.5	22.4326
IRM	101.49	0.3542	236.80	0.3546	2,786.3	22.4326
ARM	161.51	0.4573	360.69	0.4562	6,616.9	22.5398
FISH	137.17	0.3542	251.76	0.3546	23,849.5	22.4326
DRM	83.39	0.3544	203.15	0.3595	2,895.1	22.46